

**Feasibility Study for a Robotic Platform and Suite of
Sensors to Identify Degradation
in Non-Conforming Driscopipe® 8000**

Public Final Report

DoT AGREEMENT #693JK32010006POTA

Submitted to
PHMSA/DoT

Submitted by

Northeast Gas Association/NYSEARCH
20 Waterview Blvd
Parsippany, NJ 07054
<http://www.northeastgas.org>

Daphne D’Zurko
Vice President RD&D, NGA
Executive Director, NYSEARCH

Phone: 973-265-1900
Email: ddzurko@northeastgas.org

Date of Report
February 28, 2023

"LEGAL NOTICE

This Feasibility Study report is one of a series of reports on studies sponsored and/or managed by Northeast Gas Association ("NGA") that are designed to evaluate whether certain technology or engineering developments have application to the gas industry. This study was performed by an independent contractors.

Neither NGA, nor any of its members, warrant directly or indirectly, in any way or in any manner, the accuracy of the information contained in this study report or whether the technology or engineering development that is the subject of the study report has application to the gas industry.

NGA, its members, and those acting on behalf of NGA, hereby expressly disclaim any and all liability, responsibility, damages or claims, of any kind or any nature, that may result from the use of this study report, or the information contained therein. Any individual, corporation or other entity which uses this study report or the information contained therein, does so at its own risk, without reliance on the fact that NGA and/or its members sponsored this study report. Such individual, corporation or other entity assumes any and all liability that may result from its use of this study report and or the information contained therein.

This research was funded in part under the Department of Transportation, Pipeline and Hazardous Materials Safety Administration's Pipeline Safety Research and Development Program. The views and conclusions contained in this document are those of the authors and should not be interpreted as representing the official policies, either expressed or implied, of the Pipeline and Hazardous Materials Safety Administration, or the U.S. Government."

1. EXECUTIVE SUMMARY

For over fifty years, plastic pipes made of medium- and high-density polyethylene (PE) are the predominant pipes used by the natural gas industry for underground distribution network purposes. As these pipes age, it is becoming increasingly critical to ensure their integrity and longevity through routine in-service inspections. While a number of methods have been developed for the non-destructive evaluation (NDE) of these pipes from the outside, in-line inspection under live conditions and over long ranges is the preferred method as it has the potential to provide the most reliable information on pipe condition at lower cost. Additionally, the NDE inspection method must: a) be relatively fast, b) provide reasonably fine resolution inspection data, and c) be mounted on and carried by a mobile robot unit specifically-designed for traversing the interior of such pipes. Any sensor designed for this application must also accommodate pipes with relatively small diameters (i.e., ≤ 4 "), which necessitates "sensor miniaturization" and adaptability. Such systems do not exist today. To this end, a Phase 1 feasibility study was undertaken to develop concepts for a robotic platform that would carry NDE sensors for the live, long-range, non-destructive testing of PE pipes. Three distinct nondestructive evaluation (NDE) methods were explored in some detail, namely: microwave and millimeter wave imaging; terahertz (THz) imaging and spectroscopy; and ultrasonics. The robotic platform work was carried out by Invodane Engineering IE (an Intero Company), while the sensor work was carried out by the Center for Non-Destructive Evaluation at Iowa State University (ISU).

In the natural gas distribution network 2-inch diameter pipes represent around 70% of the installed pipes. The 4-inch is the second largest installation base with about 22% of the total of 742,115 miles installed. The focus on 2-inch and 4-inch pipes will therefore have the biggest impact in addressing the inspection needs for plastic pipe. The two-inch pipe does at the same time represent a bigger challenge than the four-inch one in developing an inspection system due to the small space available in the pipe. Considering that the inspection system must travel inside the pipe while applying only minimal forces to the pipe wall, so no damage will occur during the inspection process, is another challenge this development has to consider. Although plastic pipes do not suffer from the same degradation mechanisms as steel pipelines, there is still a need to uncover damages from third parties, degradation related to specific resins and extrusion methods, and other integrity threats.

NGA/NYSEARCH and InvoDane Engineering (in collaboration with PipeTel; a service-provider of inspection services, both Intero Companies) have had great success in developing commercially successful internal inspection platforms and sensor systems for unpiggable steel pipelines in the form of the Explorer iLi series of robotic inspection tools. However, there are several challenges associated with plastic piping systems that will require alternate approaches, research, and experimentation. Inline pipeline inspection systems have generally been for larger diameter, higher pressure steel transmission pipe. Using batteries, and other onboard systems, is very challenging due to the small diameters involved. Traction will also pose new challenges due to the smoother, yet more malleable surface, in addition to the potentially higher likelihood of ovality issues. The range and types of fittings to be negotiated will also have an impact on system design, including on navigation requirements.

This project is focused on developing concepts for the eventual design and commercialization of a 2"-visual-inspection-only and a 4"-with-NDE-sensors robotic systems for the inspection of plastic PE pipes. The development work of this phase has shown promising result, demonstrating that a camera based system can be deployed in 2-inch diameter pipe under live conditions and for relative long ranges for visual inspection purposes. The next phases should focus on understanding the ultimate deployable range of the system in conjunction with its detailed design.

The development work of the 4-inch-with-NDE-capabilities inspection system has also shown promising results indicating that such a system can be successfully deployed in 4-inch diameter pipe under live conditions, for relatively long ranges, carrying an NDE sensor for the detection of defects and features on a plastic pipe, including degradation experienced in non-conforming Driscopipe 8000. The modular inspection vehicle would be capable of carrying any sensor system that would fit in the available module size and power budget. The next phases should focus on understanding the ultimate limitations of the system while the detailed design is completed.

Regarding the NDE technologies that have the potential to provide sensory capabilities for the 4" system, the critical design aspects and performance of the three NDE methods stated earlier as well as their ultimate potential efficacy for this application were determined. The approaches and the outcomes of this investigation indicated that each of these three NDE methods has its own unique advantageous features as well as limitations. Moreover, sensor design miniaturization introduces certain unique design and application constraints that are not of concern in most other applications. As part of the sensor miniaturization efforts some design adaptations were considered

and implemented.

Terahertz (THz) time-resolved imaging performed well for the purpose of this project: it successfully detected all synthetic and naturally occurring defects embedded in the test samples with relatively fine temporal and spatial resolutions, and showed to be capable of detecting delamination against a simulated backfill soil environment outside of the pipes. Based on these results Terahertz imaging should be a strong contender to be considered for Phase 2, where the conceptual design showed inspection of 4"-diameter pipe size is feasible with sufficient detection performance while satisfying minimum inspection speed requirement.

In considering a possible ultrasound-based solution, three approaches were considered: captured water column fluid-coupled probes, gas-coupled probes, and dry-coupled roller probes. The fluid-coupled and gas-coupled probes did not fulfil inspection requirements, whereas dry-coupled probes met baseline requirements. Testing of commercial dry-coupled probes on pipe samples with engineered and naturally occurring defects demonstrated adequate sensitivity to the defects and good flaw depth resolution, while offering design leeway for improvements.

In developing a framework for a microwave-based NDE solution, several constraints such as size of sensor, power consumption, pipe wall thickness and type of flaws in the pipes, and the commercially available components were considered. A commercial radar-on-chip solution operating at 24 GHz was considered. A prototype single sensor module for the inspection of HDPE pipes with 4" diameter and larger was designed, built, and tested. This microwave sensor exhibited difficulties in identifying delamination on the outer surface of a pipe.

2. TABLE OF CONTENTS

1. Executive Summary	3
2. Table of Contents	6
3. Table of Figures	9
4. Table of Tables.....	12
5. Background.....	13
6. Introduction	16
7. Work scope.....	19
Task 1.1: Define Important Parameters.....	19
Task 1.2: Collaboration with the Sensor Developer.....	22
Task 1.3: Develop concepts for analysis and testing.....	24
3-A: Power system	24
3-B: Propulsion (drive) system.....	25
3-C: Communication system	26
3-D: Control/navigation system.....	26
Task 1.4: Milestone Review Meeting.....	26
Tasks 1.5.1-1.9.1: 2-inch-camera-only-system.....	27
Task 1.5.0: Concept development 2-inch camera only	27
Task 1.5.1: Analyze concepts developed – Power systems	28
Task 1.6.1: Analyze concepts developed – Drive systems	28
Task 1.7.1: Analyze concepts developed – Communication systems.....	30
Task 1.8.1: Analyze concepts developed – Control/navigation systems	30
Task 1.9.1: Define an integrated platform in a specific size.....	31
Tasks 1.5.2-1.9.2: 4-inch-with sensors-system.....	31
Task 1.5.2: Analyze concepts developed – Power systems	32
Task 1.6.2: Analyze concepts developed – Drive systems	32
Task 1.7.2: Analyze concepts developed – Communication systems.....	32
Task 1.8.2: Analyze concepts developed – Control/navigation systems	33

Task 1.9.2: Define an integrated platform in a specific size.....	34
Task 1.10.1: Conclusions - 2-inch-camera-only-system.....	34
Task 1.10.2: Conclusions - 4-inch-with NDE sensors-system.....	34
Task 2.1: Field Inspection Issues and challenges (for sensor System)	35
Task 2.2 Collaboration with the robot developer.....	35
Task 2.3: Feasibility Study Planning	36
Task 2.4: Initial NDE Sensor System Specifications	37
Task 2.5: Technology Review – NDE Sensor Techniques.....	39
Task 2.6: Milestone Meeting for Technology Review.....	39
Task 2.7: Feasibility and Design Study – THz Imaging and Spectroscopy.....	42
2.7.1 Task 2 7.1 Miniaturization Challenges	42
2.7.2 Task 2 7.2 Property and Benchmark Measurements	44
2.7.3 Task 2.7.3 Design Optimization by Simulation	54
2.7.4 Task 2.7.4 Hardware Availability - Market Survey	55
2.7.5 Task 2.7.5 Enhancement by Post-Processing	56
Task 2.8: Feasibility and Design Study - Microwave/Millimeter Wave Imaging.....	57
2.8.1 Task 2 8.1 Design Optimization by Simulation	58
2.8.2 Task 2,8.2 Experimental Verification	61
2.8.3 Task 2 8.3 Imaging Algorithm Optimization	67
2.8.4 Task 2.8.4 Build Bench-Top Prototype Building Block	67
2.8.5 Task 2.8.5 Design Specifications Study	70
Task 2.9: Feasibility and Design Study - Ultrasonic Inspection Methods.....	70
2.9.1 Task 2.9.1 Ultrasonic Materials Property Measurements	71
2.9.2 Task 2.9.2 Benchmark Measurements	72
2.9.3 Task 2.9.3 Survey Available Commercial Components	78
2.9.4 Task 2.9.4 Design Study	78
Task 2.10: Data Post-Processing, Integration and Sharing Among the NDE Sensors.....	81
Task 2.11: Final NDE Sensor(s) System Specifications	82
Task 2.12: Conclusions and Recommendations	82
8. Impact from the research results	84
9. Recommendation for future work.....	85

10. Final financial section.....	86
11. Acknowledgments	87
12. References.....	88
13. Appendix 1	90

3. TABLE OF FIGURES

Figure 1: Sample of Degraded Pipeline with Defects	17
Figure 2: Illustration of decreasing space for battery with decrease pipe diameter.	24
Figure 3: Flow loop for testing of basic concept.	29
Figure 4: Cameras tested for integration on 2”-camera-only-system.....	31
Figure 5: Site layout for communication test.....	33
Figure 6: The conceptual shape of the train-like robot module.....	36
Figure 7: The SWG defects: internal and external degradations and contamination	40
Figure 8: Examples of sample inventory containing natural and engineered defects.	41
Figure 9: Conceptual illustration of a THz array system mounted in a robot train.....	43
Figure 10: ISU-CNDE’s pulsed THz imaging system performs two-axis planar mode (left) and rotary mode (right) scans on pipe sample from inside out.	44
Figure 11: Two views of sample #1.	45
Figure 12: Examples of A- and C-scans for a 1/8” flat-bottom hole in sample #1.	45
Figure 13: Examples of A- and C-scans of a 1/4” flat-bottom hole in sample #1.....	46
Figure 14: Three slot cuts (left) and one square roughened area (right as enclosed) made on sample #2.....	46
Figure 15: B- and C-scans show all five 3/8” FBHs in Sample #3	47
Figure 16: Sample #4 has three shallow FBHs and two taped.	47
Figure 17: Planar scan performed on sample #4.....	48
Figure 18: A- and B-scan identify the three FBHs on sample #4.....	48
Figure 19: Sample #6 (left) and the experimental setup (right).....	49
Figure 20: The three slots on sample #6 (left) with low-amplitude on C-scan (right).	49
Figure 21: External degradation in the form of high-density blisters on sample #8.	50
Figure 22: THz rotational scan performed on sample #8.....	50
Figure 23: A- and C-scan results on sample #8	51
Figure 24: A- and C-scan results on sample #8 optimized	51
Figure 25: Simulating field environment by attaching a backfill soil patch to pipe surface	52
Figure 26: A- and C-scan results on sample #8 with simulated backfill soil	53
Figure 27: Setup and C-scan results for sample #9.	53
Figure 28: C-scan results for sample #10.....	54
Figure 29: A miniaturized erbium-doped femtosecond fiber laser head made by IMRA.....	55
Figure 30: Micro-Z: a handheld spectrometer as one of earliest miniaturized THz system [3] ..	56
Figure 31: A 4-wing rotary involute delay stage for fast data acquisition rate [3].....	56
Figure 32: CST Studio Suite® simulation model for detecting delamination in HDPE pipes using an open-ended waveguide probe.	58
Figure 33: Simulated reflection coefficient (S11) for a delamination with a diameter of 19 mm and a depth of 6.12 mm, shown in the complex (real-imaginary) plane. The reflection coefficients change clockwise as frequency increases from 18 to 26.5 GHz.	59
Figure 34: Simulated magnitude of reflection coefficient (S11), at an operating frequency of 24 GHz, for three delaminations with diameters of 9, 13, and 19 mm and a depth of 6.12 mm, as a function of sensor distance from the delamination center.....	60
Figure 35: Simulated magnitude of reflection coefficient (S11) at 24 GHz for three delaminations with diameters of 9, 13, and 19 mm, as a function of sensor distance from	

delamination center: (a) delamination depth of 2 mm, (b) delamination depth of 3 mm, and (c) delamination depth of 5 mm.....	61
Figure 36: Picture of scan setup using a K-band (18-26.5 GHz) open-ended rectangular waveguide probe and an HDPE pipe section (sample 3) containing FBH.....	62
Figure 37: Measured reflection coefficient (S11): (a) magnitude-phase and (b) real-imaginary forms, when scanning three FBHs using a K-band (18-26.5 GHz) open-ended rectangular waveguide probe.....	62
Figure 38: B-scan SAR images of the FBHs in sample 3. Z-axis represent depth within the pipe wall and Y-axis represent axial scan path along the pipe wall.....	64
Figure 39: C-scan raw (data) images of the FBHs in sample 3. X-axis represent scan path along the circumference of the pipe and Y-axis represent axial scan path along the pipe wall.....	64
Figure 40: Picture of scan setup using a K-band (18-26.5 GHz) open-ended rectangular waveguide probe and a sample containing FBH on a bed of sand. Three separate foreign objects were placed behind the pipe (i.e., on outside wall) representing various external discontinuities.....	66
Figure 41: C-scan raw images at 24 GHz of FBHs in sample 3 when three different foreign objects are placed behind the pipe (i.e., on outside wall).....	66
Figure 42: C-scan SAR images using wideband data of FBHs in sample 3 three different foreign objects are placed behind the pipe (i.e., on outside wall).....	67
Figure 43: Pictures of the prototype sensor module with caliper showing dimensions in mm.	68
Figure 44: Picture of the experimental setup showing the prototype sensor module being used to scan a section of sample3 and the resulting SAR image.....	69
Figure 45: Picture of a section of sample 1 and the resulting SAR image obtained using the prototype sensor module.....	69
Figure 46: Picture of a section of sample 2 and the resulting SAR image obtained using the prototype sensor module.....	69
Figure 47: Typical A-scan showing first and 2nd backwall echoes using longitudinal wave probes at 5MHz. The time delay between echoes and the pipe sample thickness determine longitudinal wave velocity.....	71
Figure 48: A-scan of shear wave first (blue trace) and 2nd (orange trace) back wall echoes using a 5MHz shear wave probe. Note that an increase of 20dB was needed to capture the 2nd back wall echo, demonstrating significant shear mode attenuation.	72
Figure 49: Pocket UT hand-held scanner with remote pulser/receiver/display unit and toller probe and cables.....	73
Figure 50: Hand scan results on FBH samples, showing B-scan results. Intensity of color is amplitude of received signals, position vertically indicates FBH depth.....	74
Figure 51: Diagrammatic view scanner setup for examining the SWG external blister samples, with roller probe moved along the length of the sample, with a rotator turning the sample. This is referred to as a X-q scan.....	75
Figure 52: Photograph and roller probe C-scan results of SWG sample #10, showing response from outer skin blisters and regions with residual response from previous tape coverage.....	75
Figure 53: Roller probe C-scan results of SWG sample #8, showing response from outer skin blisters and regions with residual response from previous tape coverage.....	76
Figure 54: Diagrammatic view of immersion scanning setup, using focused 10MHz probe	

focused on OD of pipe at blisters. 77

Figure 55: Immersion Scanning results on Sample 10 (as in Fig. 9.2-5), showing similar by higher fidelity image as compared to roller probe. 77

Figure 56: Pocket UT wheel probe scan using a single piezo element in a pulse-echo configuration, imaging FBH's of 1/4, 3/16, and 1/8 inch diameters at various depths., demonstrating that the roller probes should be able to incorporate additional piezo elements to increase scan coverage per roller probe. 81

4. TABLE OF TABLES

Table 1: Overview of Plastic Pipe Installation.	18
Table 2: Initial System Characteristics.....	20
Table 3: ASTM D3035 Standard for Plastic Pipe; focus for this work highlighted in yellow.....	23
Table 4: The initial specifications for both NDE sensors and robot modules.....	38
Table 5: Summary of suppliers of commercial components for considered ultrasound approaches.....	78

5. BACKGROUND

As plastic pipes are increasingly used to convey natural gas underground, the status of their working condition in the field has become critically important to the natural gas industry, and has been a focus of government regulations [1]. Measurement modalities are being sought to effectively and efficiently inspect the massive pipeline systems and to obtain the most accurate and complete information about the pipes' longevity and integrity. Particularly, it is necessary to be able to perform the inspections from the inside of the pipes after installation using techniques developed in the field of nondestructive evaluation (NDE). For this, robotic mobile units capable of carrying NDE sensors are being considered to perform such internal inspection.

In the last 20 years, NYSEARCH and InvoDane Engineering/PipeTel (now part of Intero) have had great success in developing commercially successful internal inspection platforms and sensor systems for unpiggable steel pipelines in the form of the Explorer iLi series of robotic inspection tools. From the commercialization of Explorer 10/14 in 2010 to the availability of Explorer 6 in 2020, PipeTel operates Explorer iLi robots that can inspect 6-inch to 36-inch unpiggable steel pipelines under live conditions.

While the plastic distribution main infrastructure is generally newer than the steel infrastructure, PE has been the current material of choice in lower pressure distribution applications for several decades now. With the aging of the infrastructure some older plastic pipes have shown signs of degradation. Thus, the operators of plastic distribution piping networks would benefit from the availability of an internal inspection platform that can provide integrity inspections with minimal excavation and customer disturbance, similar to what is available for steel pipelines. Although plastic pipes do not suffer from the same degradation mechanisms as steel pipelines, there is still a need to uncover damages from third parties, degradation related to specific resins and extrusion methods, and other integrity threats.

InvoDane Engineering has a long and successful 20-year history in the development and operation of complete robotic pipeline inspection platforms for buried steel pipelines. As such, much of the existing expertise will be applicable to the development of a plastic pipe inspection platform as there are many similarities. However, there are some different challenges associated with plastic piping systems that will require alternate approaches, research, and experimentation. Inline pipeline inspection systems have generally been for larger diameter, higher pressure steel

transmission pipe. Plastic piping is only used for distribution pipe. The range of plastic piping systems will, in general, be significantly smaller in diameter than the steel transmission piping, which may pose challenges for smaller platforms when it comes to available space for batteries and other components. Platforms for smaller diameter pipelines may also pose higher cross-sectional obstruction to flow. Traction will also pose new challenges due to the smoother, yet more malleable surface, in addition to the potentially higher likelihood of ovality issues. Communication and control may require a different approach as the pipeline will no longer act as a wave guide for wireless signals and the mission profile will likely be different with distribution related pipeline configurations as opposed to transmission related. The range and types of fittings will also have an impact, including on navigation requirements.

The Center for Nondestructive Evaluation (CNDE) at Iowa State University (ISU), a leading NDE research organization, was tasked to identify NDE technologies suitable to the application in hand. After a careful assessment of available NDE technologies three techniques, namely microwave and millimeter wave imaging, terahertz imaging and spectroscopy, and ultrasonics, were selected as the potential candidates for the NDE sensor.

Microwave and millimeter-wave synthetic aperture radar (SAR) 3D imaging utilize electromagnetic signals in the frequency range of ~300 MHz to 300 GHz (corresponding to a wavelength range of 1000 mm to 1 mm). Signals at these frequencies easily penetrate inside dielectric materials such as PE, providing high resolution images of their inner structures. Advanced and unique millimeter-wave imaging systems have been designed for NDE applications. A non-contact microwave/millimeter wave circumferential array (ring of probes) that can be mounted on a robot to image a PE gas pipes from the inside is explored. Design challenges that were investigated as part of this work are hardware miniaturization techniques and thermal considerations. These challenges become significant at higher frequencies (>40 GHz), at which performance in defect detection increases, where integrated miniaturized integrated circuit (IC) systems are of limited commercial availability. Given the space limitations in this application the use of lower frequency systems, which can be miniaturized, is necessitated.

In recent years, terahertz imaging and spectroscopy (THz) has emerged as a new and powerful technology for material characterization and inspection in a variety of applications in science and engineering, including automotive, aviation, food, energy, materials, pharmaceuticals, medical

diagnosis, forensics, defense, and homeland security. Residing in-between microwave and mid-infrared, typically ranging from 50GHz to 10 THz, in the electromagnetic spectrum, THz has exceptional 3D resolution for NDE imaging applications. Currently, under separate NYSEARCH/NGA funding, THz has shown particularly promising results for inspecting PE plastic pipes. Thanks to its spatial resolution, THz is able to resolve sub-millimeter defects as well as the distribution of the delamination layers in non-conforming Driscopipe 8000 at high definition. In this project, miniaturizing the sensor for interior pipe inspection is expected to be the most challenging task. As the newest technology among the three proposed here, THz's product development is still at the early stages; however, new innovations are emerging rapidly.

Ultrasonic inspection of pipes via pigs has been used for several decades in liquid-filled pipes but is less mature in applications with gas-filled pipes. Fluid filled plugs or captured water columns like the ISU-CNDE developed Dripless Bubbler [2], gas coupled probes or dry couplant films are seen as possible solutions to achieve consistent coupling between the pipe wall and probe, with each having unique advantages and disadvantages. Maintaining a constant and uniform coupling condition while scanning will be the challenge, considering distorted pipe bores, bends/sweeps, weld sprue and foreign material in the pipe bore. Changing ambient pressure conditions in the pipe will have the greatest effect on a gas coupled approach, where probes are designed to operate most efficiently at particular couplant acoustic impedances (the product of density and velocity of the coupling medium). Miniaturization of gas probe elements will also be challenging.

6. INTRODUCTION

Driscopipe is a type of high density polyethylene plastic pipe used in the natural gas distribution system since the 1960s. Driscopipe type @8000 pipe was produced from the late 1979 through 1997 and was installed for another few years following termination of production. The pipe was available in sizes from ¼” to 8” in diameter.

In March 2012, PHMSA issued an Advisory Bulletin alarming operators using this type of pipe of potential material degradation that was identified in such pipes installed between 1978 and 1999 in desert-like environments in the southwestern United States, namely Arizona and Nevada. In November 2013, Performance Pipe, a division of Chevron Phillips Chemical Company and the manufacturer of the pipe, published a report on the findings of an engineering analysis and tests conducted to identify the source of the problem. The report stated that the cause of the degradation is thermal oxidation of the pipe, the potential of which advances with increased temperature of the pipe and increased time at the elevated temperature conditions. The report recommended that *“operators in the highest temperature regions, such as the desert southwest and southern most regions of the United States may want to inspect and sample a broader portion of their system in conjunction with the risk ranking.”*

To the naked eye, the degraded pipe displays delamination or peeling on the outer surface and a crumbling appearance with many cracks on the inner surface of the pipe (see **Figure 1**). Under a microscope (see Figure 1), microcracking of the material is clearly seen.

A number of limited efforts have tried to identify technologies that would be able to inspect from the inside or the **outside** of the pipe with limited success. Acoustic technologies were tried and eliminated as impractical. Ultrasonic technologies (GE USM-Go+ system) were tried and proved effective for inspection from the outside of the pipe. However, it requires excavating and exposing the pipe, which is not practical, if long segments of the network are to be inspected. When tried from the inside of the pipe, the need of a liquid couplant rendered the

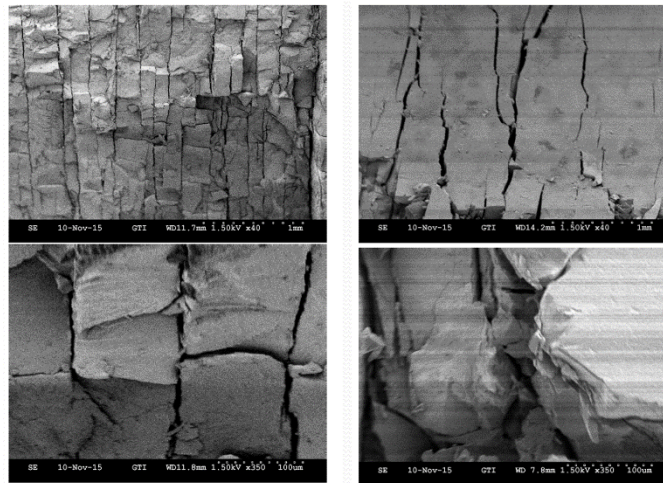


Figure 1: Sample of degraded pipes with defects and Scanning Electron Microscopy images of degraded pipes

ultrasonics-based system impossible to use under live conditions. Camera technologies were also tried for internal use but were abandoned as providing very limited operational range in addition to facing other operational issues.

The industry is therefore in need of a tool that will: 1) allow insertion of a sensing element in a live pipe, 2) detect delamination in Driscopipe @8000 pipes, 3) operate in a live distribution main and travel long distances, 4) negotiate obstacles encountered in the typical distribution network, such as bends and tees, and 5) identify/detect other defects that may be present on the pipe wall. It should be able to operate without a tether and be controlled by the operator wirelessly while having enough power to provide for a log range. A system with such capabilities was successfully developed, by NYSEARCH/NGA with cofunding from PHMSA, over the last (15) years for metallic transmission natural gas pipelines. In this project we bring all the accumulated expertise

and success into this effort in order to develop such an in-line system for natural gas plastic pipes.

The installation of plastic pipe for the natural gas distribution network has increased over the last few decades. The main material used is PE with 2-inch diameter pipes representing around 70% of the installed pipes. The 4-inch is the second largest installation base, with 22% of the total of 742,115 miles installed, as seen in **Table 1**.

Table 1: Overview of Plastic Pipe Installation.

Plastic	Unknown	<=2"	<=4"	<=8"	<=12"	>12"	Total
PVC	12	9,031	1,382	43	0	-	10,468
PE	268	517,843	169,240	52,014	1,669	82	741,115
ABS	-	2,593	358	0	-	-	2,950
Other	2	74	74	4	-	-	155
Total	282	529,541	171,054	52,061	1,669	82	754,688

Plastic Mains - Annual Gas Distribution Report PHMSA 2018

The focus on 2 and 4-inch will therefore have the biggest impact of addressing the inspection need for plastic pipe. The smaller pipe does at the same time also represent the biggest challenge in developing an inspection due to the small space available in the pipe. Considering inspection system must travel inside the pipe with applying only minimal forces to the pipe wall so no further damage will occur during the inspection process is another challenge this development has to consider.

7. WORK SCOPE

The workscope description is organized according to the “*Team Project Activities*” outlined in Attachment 1 of the proposal (as approved by PHMSA). The task and sub-task numbers are consistent with that list of activities.

Tasks 1.1 through 1.10 were carried out by Invodane Engineering while Tasks 2.1 through 2.12 were carried out by Iowa State University. Given the decision of the funders at the first Milestone Meeting to pursue two different platforms (not envisioned when the proposal was written and accepted), two parallel efforts were carried out for platform development. As a result, Tasks 5-10 have been reorganized as Tasks 5-1 – 10.1 for the 2:-camera-only platform development effort and Tasks 5.2 – 10.2 for the 4”-with-NDE-sensors platform development effort.

TASK 1.1: DEFINE IMPORTANT PARAMETERS (for robotic system)

The starting point for the development of the robotic system was a set of desired system characteristics/capabilities obtained through initial discussions with the natural gas industry personnel involved in this project, as shown in **Table 2**. The importance of each capability is identified by a color, green being the “most important”, blue “less important”, and yellow “nice to have”.

Table 2: Initial Robotic System Characteristics.

SYSTEM CHARACTERISTICS		IMPORTANCE	Bi-Directional Operation		
Pipe Material	HDPE		Tetherless		
	MDPE		Live Control of Robot		
Pipe Diameter SDR 11	1"		Range of Robot	500 ft	
	1.25"			1,000 ft	
	2"			2,500 ft	
	4"			5,000 ft	
	6"		Inspection speed	500 ft/hr (2"/s)	
	8"			1,000 ft/hr (4"/s)	
Operating Pressure	60psi			2,500 ft/hr (10"/s)	
	124 psi		Video camera	Live Feed (1fps)	
Launching	Vertical Saddle			Live Feed (30fps)	
	Angled Saddle			Recorded images	
Live Inspection			Defect Detection	Delamination	
Obstacles Negotiation	Vertical Segments			Foreign objects in material/joints	
	Inclined Segments			Gouges/Mechanical Damage	
	Bends			Cracks	
	Tees			Cold Butt Fusion	
	Reducers - Stiffeners			Defective electrofusion	
	Fusion joints			Able to handle liquids in Pipe	
	Valves		Gas flow rate effect		

These initial set of system characteristics/capabilities was discussed and approved by the funders at the initial project kickoff meeting in February 2021. Following are further details on the desired features of the robotic system.

Pipe Material: The inspections are to be done in High-Density Polyethylene (HDPE) and Medium-Density Polyethylene (MDPE) pipes.

Pipe Diameter: The pipe diameters dictate the capabilities of the robot. The agreed upon diameters for inspection were 2-inches and larger, while also considering smaller diameters when producing concepts.

Operating Pressure: Standard operating pressure of the pipeline is 60 PSI, while higher pressures up to 124 PSI were to be considered during the design process.

Launching: The launching process involving tapping the pipe and release of the robot into the pipe was agreed to be done at an angle.

Live Inspection: Inspection of the pipeline needs to be carried out under live conditions.

Range of Robot: It was determined that we should consider ranges of about 1000 feet (or higher, if possible).

Inspection Speed: Based on current inspection robot designs and detection requirements for MDPE and HDPE inspections, the maximum speed of the robot would be 2"/sec.

Video Camera: A video camera (if not more) will have to be integrated onto the system with a live video feed sent back to the operators at the video speeds up to 30 frames per second (fps). This would allow for immediate feedback to pipe conditions and areas of interest. In combination with the live video feed requirement, the camera images are to be saved on board the robot.

Defect Detection: The main defect to be detected with the system was determined to be delamination of the internal pipe wall. Additional defects are to be detected with the non-destructive evaluation sensors onboard.

Able to handle liquids in pipe: The pipes used in the distribution system often contain liquids. The inspection systems should not be compromised by the presence of liquids.

Gas flow rate effect: Because the pipelines are going to be in use during the inspection, there should not be any significant restriction of flow due to the robot's cross-sectional area.

It has to be noted that during project development additional requirements were further added as design considerations which are as follows.

Odometry: Knowing the location of the robot within the pipe is extremely important. Therefore, an odometer is required to correlate the distance travelled down the pipe with important defect/features detected.

Emergency Removal: Due to the need to provide live inspection, additional considerations for removal of the robot in case of emergency without disrupting the flow of gas have to be taken into account.

Pipe Deformation: Since the pipe to be inspected is MDPE or HDPE it may deform under high loads. Therefore, the inspection robot must not apply significant force onto the interior walls, which may cause permanent damage to the pipe.

Separately, several hardware requirements were decided and outlined as follows.

Size: Due to the size of the pipe, all hardware must be small enough to fit within the robot.

Power: Power supply should be adequate to provide a range for the system of up to 1,000 ft (or higher, if possible).

Image Quality: it should be high enough for the visual detection of important defects while the robot is travelling at 2" per second.

Branch Detection: It was agreed that another important area of focus for detection was location of branches in the pipeline. These branches should be visible by the camera and should be easily

located using odometry.

As a result of these initial specifications, from a design point of view the key parameters to work with included the following:

- Sensor size, weight and number of modules
- Power requirements
- Drag force from sensor
- Pipe alignment needs for sensor
- Sensor contact or proximity with pipe wall
- Live communication
- Calibration required
- Data storage required
- Initial size and weight target

Notice that many of these key design parameters involve characteristics of the sensory system, which required input from the sensor developer.

TASK 1.2: COLLABORATION WITH THE SENSOR DEVELOPER

The sensor development, carried by ISU in parallel to the platform development effort, focused on three different technologies; microwave, ultrasound with dry-coupling, and terahertz. Each of these have different requirement for power, sensor size and number of modules, support electronics, as well as data storage requirements.

A high-level guideline for these three sensing technologies in terms of their power and other operational parameters was developed by ISU early on during the project and were used in developing the early concepts.

Based on the knowledge we have from other development work of the same nature the target pipelines were identified to be diameters of 1.0 to 8 inch and schedule DR15 or DR17 (shown in **Table 3** in the yellow box).

Table 3: ASTM D3035 Standard for Plastic Pipe. The focus for this work highlighted in yellow.

Dimensions of PE pipes according ASTM D3035 Standard Specification for Polyethylene (PE) Plastic Pipe (DR-PR) Based on Controlled Outside Diameter.

Nominal Pipe Size (in)	Outside Diameter (in) (mm)	Min. Wall Thickness (in) (mm)									
		DR 32.5	DR 26	DR 21	DR 17	DR 15	DR 13.5	DR 11	DR 9.3	DR 9	DR 7
1/2	0.840	0.062	0.062	0.062	0.062	0.062	0.062	0.076	0.90	0.093	0.120
3/4	1.050	0.062	0.062	0.062	0.062	0.068	0.078	0.095	0.113	0.117	0.150
1	1.315	0.062	0.062	0.063	0.077	0.084	0.097	0.120	0.141	0.146	0.188
1 1/4	1.660	0.062	0.064	0.079	0.098	0.107	0.123	0.151	0.178	0.184	0.237
1 1/2	1.900	0.062	0.073	0.090	0.112	0.123	0.141	0.173	0.204	0.211	0.271
2	2.375	0.073	0.091	0.113	0.140	0.153	0.176	0.216	0.255	0.264	0.339
3	3.500	0.108	0.135	0.167	0.206	0.226	0.259	0.318	0.376	0.389	0.500
4	4.500	0.138	0.173	0.214	0.265	0.290	0.333	0.409	0.484	0.500	0.643
6	6.625	0.204	0.255	0.315	0.390	0.427	0.491	0.602	0.712	0.736	0.946
8	8.625	0.265	0.332	0.411	0.507	0.556	0.639	0.784	0.927	0.958	1.232
10	10.750	0.331	0.413	0.512	0.632	0.694	0.796	0.977	1.156	1.194	1.536
12	12.750	0.392	0.490	0.607	0.750	0.823	0.944	1.159	1.371	1.417	1.821
14	14.000	0.431	0.538	0.667	0.824	0.903	1.037	1.273	1.505	1.556	2.000
16	16.000	0.492	0.615	0.762	0.941	1.032	1.185	1.455	1.720	1.778	2.286
18	18.000	0.554	0.692	0.857	1.059	1.161	1.333	1.636	1.935	2.000	2.571
20	20.000	0.615	0.769	0.952	1.176	1.290	1.481	1.818	2.151	2.222	2.857
22	22.000	0.677	0.846	1.048	1.294	1.419	1.630	2.000	2.366	2.444	3.143
24	24.000	0.738	0.923	1.143	1.412	1.548	1.778	2.182	2.581	2.667	3.429

After discussion among all parties, the 4-inch diameter pipe was selected as the base case for the developing the initial guidelines.

With that, a typical geometrical evaluation was conducted using the 4-inch pipe as a base. The optimal length to diameter ratio of robotic modules was sought ensuring safe passage of the robot through various pipeline system features as bends and tees. With that knowledge and expanding the analysis to pipe sizes down to one-inch, a general sensor body sizing chart for different pipe diameters was developed.

Based on a similar analysis a chart was also developed for the sensor weight that the robot would be able to carry as the payload using our extensive experience from our Explorer program.

Similarly, analysis was carried out to determine the maximum allowable power requirements for the sensor module based on the available volume for on-board battery storage and the weight limitations identified earlier. It is important to keep in mind that the space available for onboard power storage decreases geometrically as a function of pipe diameter squared *i.e.*, a decrease in diameter by a factor of two, results in decrease of available space by a factor of four. It is this behavior that makes the development of smaller size platforms such a challenging endeavor.

Initial implementation in a modular configuration of the three sensor technologies considered, provided by the sensor developers, was used for developing the various platform concepts. With ISU providing initial estimates for the power consumption of each sensory system for eight-, six-, and 4-inch systems, a power budget on a per battery-module basis was developed for each pipe size. As seen, in these **initial estimates** the microwave system requires the least amount of power, resulting in the longest battery life per module, followed by the UT system. The THz system, having the highest power requirements is exhibiting the lowest battery life of all. As a result, at this stage of development, it appeared that the microwave sensing technology would be the easiest technology to implement from a power point of view, followed by ultrasound.

TASK 1.3: DEVELOP CONCEPTS FOR ANALYSIS AND TESTING

Task 3-A: Power system

Given the initial specification that we use a tetherless system (to maximize range), the source of power to drive the onboard system for an inspection will be batteries with their associated power control system. Depending on the actual concept to be selected, the batteries could be supported by an in-line charge system. The key parameter for battery sizing is directly related to pipe diameter, since the cross-section of a cycle (the cross-section of the module) decreases geometrically with the square of the diameter, as illustrated in **Figure 2**.

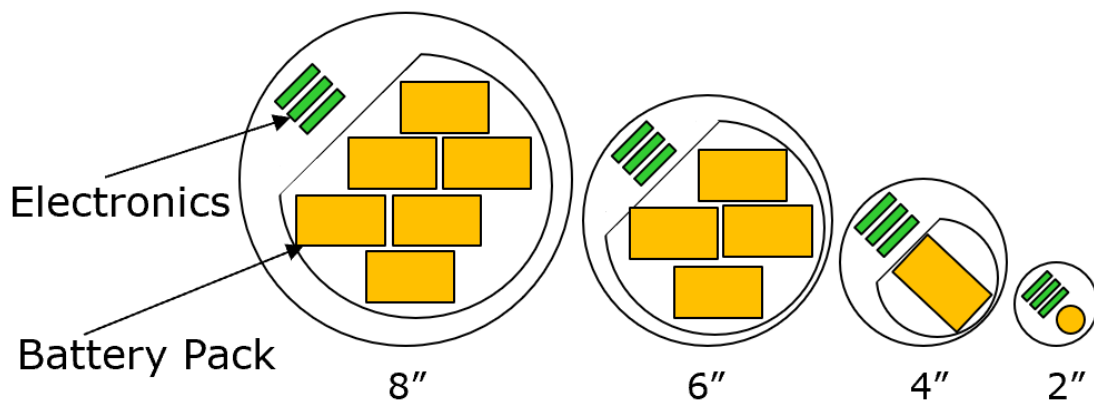


Figure 2: Illustration of decreasing space for battery with decrease pipe diameter (volumes shown in actual proportion to physical size).

The available on-board power will greatly impact the systems that can be included on-board, such as drive system, sensor system, communication system, data recorder, etc., as well as the range of operation and/or the run time of the system.

A number of concepts were explored regarding extending the range of the system by increasing the available power to the robot while in operation inside the pipe. One of the concepts considered was recharging the batteries using a wireless inline charge system. As the batteries are nearing depletion, the robot would be parked at a certain point in the pipe and a bell hole would be dug to access the pipe from the outside. The wireless charge system would be installed on the pipe right outside where the battery modules and the batteries would be charged. A high-level evaluation was performed for such a system. It was found that in this application the losses would be very high rendering the system highly inefficient. Furthermore, the onboard system would be heavy and would take up valuable space inside the robot, space required for other elements of the inspection system. At this point, it was decided that this concept would not be developed any further.

Task 3-B: Propulsion (drive) system

A number of concepts were developed for the propulsion (drive) system. After an initial review three concepts were further developed as a potential means for the robot to move down the pipe during inspection under live conditions. Each concept was evaluated and its pros and cons listed in order to allow for its selection or rejection as the system to be used.

The concept selected offers ability to be deployed reliably, has the potential to reduce the size of the drive mechanism compared to other concepts, and requires minimal control as the robot moves down the pipe. Another very attractive feature is the low (or zero) radial contact force on the pipe wall. Also, the drive system can be compact and drive in both directions with the same force.

Task 3-C: Communication system

Again, a number of concepts were developed, which following an initial review resulted in the further consideration and analysis of three concepts. These three concepts were: (a) above ground communication, (b) using the tracer wire typically found buried next to plastic pipes, and (c) using a tether. Following a detailed evaluation, it was decided that a tethered system would have to be used to provide the necessary communication between robot and operator for data transmission and control.

Task 3-D: Control/navigation system

The control and navigation requirements for the inspection system will depend on the concept selected for final development. From a navigation point of view the device will be guided by the walls of the pipeline and will travel in both directions, hence, the functionality required includes forward, stop, and reverse motions. The main input for navigation will be the camera but could also include an additional sensor device that can identify features in the pipe that may interfere with proper system functioning.

From an overall control point of view the forward, stop, and reverse motions would be key, as will be the ability to control the sensor deployment, recording, odometer etc. The onboard control system would consist primarily of a communication module, a data recorder, and an activator control module.

The above ground control station located at the operator's computer will handle the communication between operator and robot and will provide the graphic user interface (GUI) to operate the inspection system. Given our extensive experience developing GUIs for the Explorer series of robots, this task is not expected to provide any major challenges.

TASK 1.4: MILESTONE REVIEW MEETING

A milestone review meeting was held in October 2021 between the funders and the system developers (Invodane and ISU) to present the results of the work done to that date. The concepts developed for the platform (see Task 3 above) were presented and a set of initial recommendations were made to the funders. Each concept was discussed and its performance compared to the initial set of requirements adopted during the kickoff meeting in February 2021.

It was evident from the analysis of the various platform concepts presented that the concept recommended would meet a larger number of the requirements set during the project's kickoff meeting, especially for the pipe diameter range of 4" – 6" diameter. Given that the input from the sensor development effort (ISU work) was that the smallest diameter an NDE sensor could be deployed in is a 4-inch pipe, it was decided to proceed with this option. This effort was estimated to require at least three years to commercialization.

After further discussion among the stakeholders, and given the long timetable for the development of the 4" system with full NDE sensory capability, it was decided to divide the program into two parallel efforts. The first would focus on developing a 4" system with full NDE sensor capability (the sensor to be selected from among those being considered by ISU) and with a development time of about three plus years. The second would focus on a 2" pipe diameter and larger system with visual inspection capability ONLY, and with a timeframe of less than two years to commercialization. Based on this decision, a revised scope was developed and approved by the funders a few weeks after the milestone review meeting focusing on completing the concept development for the 4"-with-sensors system and initiating a concept development effort for the 2"-camera-only system. With this new divided workscope, the potential concepts for the 2-inch camera-only system were expected to be significantly different and require an additional concept development phase to identify a better solution.

TASKS 1.5.1-1.9.1: 2-INCH-CAMERA-ONLY-SYSTEM

Task 1.5.0: Concept development 2-inch camera only

As discussed earlier an additional concept development effort was introduced to the workscope to evaluate the existing concepts and develop additional ones for the revised requirements for a 2"-visual-inspection-only (camera-only) system. With this, the requirement for a non-NDE based system introduced a different series of challenges. Numerous concepts were initially developed during brainstorming sessions. Most were eliminated and a set of four final concepts was taken to further evaluation.

Two geometries for the platform were selected and fully evaluated. Both motorized and flow-driven concepts were considered. Needs to be noted that utilizing the flow to propel the

system provides for no control of the path or speed of the device as it moves down the pipe. Also, both tethered and non-tethered options were considered.

Task 1.5.1: Analyze concepts developed – Power systems

An analysis of the power requirements of such a system was carried out to determine the size of batteries to power the system over the required range. Very early on in this analysis it became evident that the communication system is the most power hungry component of such a system. The power needs of the system were then determined based on the equipment needed to be integrated onto the system.

Next a benchtop prototype was built to test the various components and verify the theoretical calculations. Because the building of 2” system requires the building of special electronics (rather expensive), a 4” system was built using off the shelf electronics. Following comprehensive testing the shape of the module was selected.

With the 4” experimental system tested and validated, the Printed Circuit Board (PCB) design for the 2-inch version was conceptualized and new functions were added. The size of the 2” system should be no more than 1.5-inch in diameter to allow for minimal pressure drop across it and to allow the system to negotiate butt fusion welds and potential ovality in the pipe. This set the limits on the allowable size of the PCB. To fit all the parts into this small volume, a Rigid-flex PCB must be used and folded like 2 PCBAs stacked up.

Task 1.6.1: Analyze concepts developed – Drive systems

Due to the size constraints of the 2-inch PE pipeline, the availability of space for an on-board drive system is extremely challenging. The two concepts developed earlier were analyzed further. One of the two concepts was found to have difficulties navigating obstacles in the pipe, such as weld beads, and was eliminated. We then proceeded to further evaluate the remaining one concept. An initial 2-inch prototype was built and tested to verify the concept’s ability to drive down a pipe without sliding. To accommodate the available hardware components a larger 4-inch prototype was designed and tested, as also stated earlier. This prototype was tested in a larger pipe to ensure it functioned the same as the 2-inch prototype, followed by the installation of all hardware.

The test setup in the laboratory was used to test the initial concept and to gather feedback for further development in an iterative fashion. When running functionality tests on the larger 4-inch prototype it was determined that the proposed control concepts would need to be used. This would allow for additional stability of the robot, but also control the speed at which the robot would move down the pipe allowing for clear video recordings. The selected control option would also allow for the system to operate in the reverse direction to allow inspection against the pipe flow and easy retrieval into the launcher. It would also allow for the removal of the robot in an emergency.

A larger-scale test of the 4-inch prototype was run in the test facility that was built in the laboratory. The piping network incorporated an adjustable fan to control the air velocity, a number of obstacles to simulate weld beads, and an integrated deployment system, as shown in **Figure 3**.

Tests were carried out to assist in evaluating all major functions on the system, including camera operating and performance parameters, and results will be presented and discussed later in this report.



Figure 3: Flow loop for testing of basic concept.

Task 1.7.1: Analyze concepts developed – Communication systems

A communication system was integrated in the 2-inch-camera-only system with the operator having control on when to turn the system ON or OFF

Task 1.8.1: Analyze concepts developed – control and navigation systems

To verify that the control system was sufficient to provide proper control and stability for the robot, it was tested with the LED and camera on to determine the quality of the resulting images.

Extensive testing was carried out under different travel speeds (in/s) and with different camera speeds (frames per second). There are tradeoffs between these two parameters and the overall resolution of pipeline detection. For example:

- If the module moves too fast and the camera is too slow, you may miss sections of the pipe
- If the module moves too slow and the camera is too fast then you have extra consumption of power by the lighting system.

The image from the onboard camera is the main data from the inspection. The quality of the image is a key operating parameter for the system, a parameter related to device speed and image resolution. Therefore, a detailed evaluation of a number of off-the-shelf cameras was carried out as seen in **Figure 4** below, each camera offering a different frame speed and data rates. The testing was carried out with using the 4-inch test system for the reasons explained earlier. The inspection speed was varied, while seven different resolutions were tested. Based on these tests a camera was selected offering the best balance of the performance parameters listed earlier.

Resolution	2640 Data Rate kbps	2640 fps
1280 x 720	2,395	12
1024 x 768	3,293	12
800 x 600	4,277	19
640 x 480	2,056	25
480 x 320	1,043	25
400 x 296	2,610	40
320 x 240	1,463	48

Figure 4: Cameras tested for integration on 2"-camera-only system.

Task 1.9.1: Define an integrated platform in a specific size.

Based on the above analysis the most promising platform and components for a 2"-camera-only system was selected, with a camera and LED system for recording visual images inside the pipe, and an SD card for allowing the option of on-board storing of the images. The system will be launched into the pipe from a launcher attached to the pipe using off the shelf fittings. A rather detailed conceptual design of the launcher system was carried out.

TASKS 1.5.2-1.9.2: THE 4-INCH-WITH SENSORS-SYSTEM

The main objective for the 4-inch inspection system is to combine a visual inspection with an NDE inspection system. As discussed earlier the 171,000 miles of 4-inch pipe represents more than 20% of the total installed pipe in the natural gas distribution system. It carries significantly more gas than the 2" system and is therefore of high importance to the overall gas network. The 4-inch system is required to run a visual inspection of the pipeline with the addition of an NDE sensor to inspect the internal pipe for defects and damage. The work and knowledge gained from the 2-inch camera-only system (task 1.5.1 to 1.9.1) may be used for the development of the 4-inch system as well. The 4" system-with-NDE is based on the design selected in Task 1.3 above.

Task 1.5.2: Analyze concepts developed – Power systems

The onboard subsystems that need power from the power system for the 4-inch-with-sensors platform would be the driver system, the onboard control system, the camera and communication systems, and the NDE sensor. All options were considered further, i.e., a power tether only system, an onboard battery only system, and a combination of tether and onboard batteries. Following detailed evaluation, the most effective option was selected.

Task 1.6.2: Analyze concepts developed – Drive systems

The drive system selected earlier was further evaluated and a number of tests were run in the test loop in the laboratory to verify its performance, reliability, and robustness.

Task 1.7.2: Analyze concepts developed – Communication systems

As discussed in Task 3-C, several options for communication were developed. The main purpose of the communication system is the control of any actuators and of image transmission. The image resolution was discussed in an earlier section. Based on the image resolution selected earlier and the control bandwidth needed for each operation, the needed communication rate was determined assuming a certain robot operational range. Since communication for this application is extremely important and there is no significant information in the literature, a comprehensive analysis was carried out via series of tests, which were carried out at an offsite location that provided a suitable set of buried pipes and wires to allow us to test the different concepts/options considered. A number of off the shelf communication hardware and software were purchased for the test.

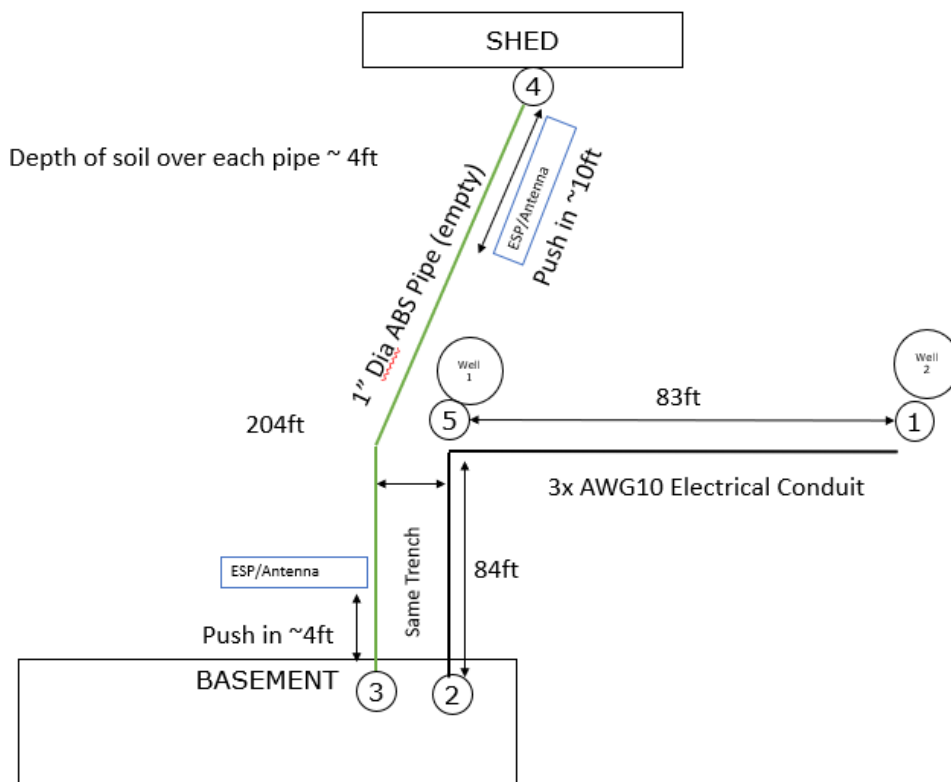


Figure 5: Site layout for communication test.

The site layout is shown in **Figure 5**. A 165 ft long conduit with 3 -10 gauge wire was laid out from position 1 via position 5 to position 2. The other installation for the test is an empty 204 ft 1-inch diameter ABS pipe, from position 3 to position 4.

A detailed test protocol was developed to test the various hardware under various conditions. The tests were executed and the results were analyzed.

Task 1.8.2: Analyze concepts developed – Control/navigation systems

The key elements for control and navigation of the 4-inch inspection system were developed in the earlier concept development stage. Those were further reviewed, analyzed, and ultimately further validated in this stage of the work.

It is pointed out that the concept selected minimizes the contact force normal to the pipe wall thus, preserving the integrity of the plastic pipe by avoiding any damage of the pipe wall.

Task 1.9.2: Define an integrated platform in a specific size.

The integrated inspection platform proposed is based on a modular approach with each module having a unique function. The platform would have at its two ends drive modules with a built-in camera on either end. The electronic modules would be next, located towards the center of the platform next to the sensor modules. If required, more modules for each one of these functions could be fitted on the platform. The connection between each module would be of a flexible nature to allow driving around bends and other features.

TASK 1.10.1: CONCLUSIONS - 2-INCH-CAMERA-ONLY-SYSTEM

The development work in this project has resulted in positive results as it has developed a promising concept for the deployment of a camera-based system in 2-inch diameter PE pipe to provide live visual inspection capabilities to detect various defects in the pipe and identify major features in the piping system infrastructure. The main components of such system are a deployable system with wheels, a launch and receive system for live operation, and a miniaturized electronic package with camera and lighting onboard. The images will be stored onboard. While it is expected that this system will have a range of 500 ft to 1,000 ft (or greater), part of the next phase work should focus on further understanding the ultimate deployable range of the system. Furthermore, the detailed design of the system needs to be completed. A test facility should be developed to facilitate the system development.

TASK 1.10.2: CONCLUSIONS - 4-INCH-WITH-NDE-SENSORS-SYSTEM

The development work on the 4-inch inspection system with NDE sensing capability integrated on it has shown promising results in our ability to design and build a platform that can be deployed in 4-inch pipe diameter under live conditions and provide detection capabilities for various defects (including delamination in non-conforming pipe) using an NDE sensor. The main components of such a system are a deployable modular platform consisting of drive modules, electronics modules, and sensor modules; and a launcher and receiver to deploy the system under live conditions.

The inspection vehicle (platform) would be capable of carrying any sensor system that would fit in the available module size and power budget. The next phase of this program should focus on understanding the ultimate limitation of the system and designing in detailed the optimum one. Finally, the detailed design of all system components needs to be completed in a future phase and extensive testing to be carried out, for which a test facility should be developed to facilitate the system development.

TASK 2.1: FIELD INSPECTION ISSUES AND CHALLENGES (FOR SENSOR SYSTEM)

The Iowa State University Center for Non Destructive Evaluation (ISU-CNDE) sensor development team, consisting of lead researchers of these three NDE techniques, met with the funders and the platform developer in the kick-off meeting that took place in February 2021 to discuss the difficulties and problems, and specify the needs for a plastic pipe field inspection system. The ISU team also presented the leading edge NDE technologies that are most suitable for addressing those inspection problems.

The knowledge gained here helped to create the initial specification list for the sensory system (see Task 2.4 below) using a technology review (see Task 2.5 below) and information obtained from NYSEARCH and SWG in which key parameters, such as diameter and thickness for PE pipes of interest, are to be included,. Furthermore, a list of flaw types, locations, and severity was to be generated as the guide for later fabricating the experimental samples in the project.

TASK 2.2: COLLABORATION WITH THE ROBOT DEVELOPER

The ISU-CNDE team worked closely with the robot developer Invodane Engineering, with NYSEARCH's participation, via a series of meetings throughout the duration of the project, to learn the current status and details of the robot unit in the following aspects:

- Robot construction and housing for NDE sensor unit,
- Mechanical and electronic interfaces with NDE sensor unit,
- Motion mechanism and stability,

- On-board data storage, processing and transfer, and
- Home (above ground) communication.

As stated above, the NDE sensor(s) are to be carried by a robotic vehicle to inspect the pipe from the inside. The robot currently under development by Invodane Engineering is conceptualized to be a series of robotic train-like module of cylindrical-like shape with length L and diameter D , as shown in **Figure 6**. The target sizes of pipe and robot modules were then selected to comply with ASTM D3035 Standard Specification for Polyethylene Plastic Pipe. The size of robot module was optimized to allow maneuvering 90°-turn within the corresponding target pipe.



Figure 6: The conceptual shape of the train-like robot module.

TASK 2.3: FEASIBILITY STUDY PLANNING

Given the information obtained from Tasks 2.1 and 2.2, NYSEARCH, the ISU team, and the robot developer Invodane Engineering worked to identify key issues and challenges on which to focus in this feasibility study, including the following areas:

- NDE sensors' size, weight and power consumption,
- NDE scan issues associated with pipe geometry, e.g., pipe size and shape variation, turn curvature,
- Type of flaws of interest (i.e., delamination, cracks, voids, butt joint lack of fusion, etc.)
- NDE scan capability and stability issues associated with robot motion,
- The effect of natural gas composition and flow on NDE sensor performance,
- Issue related to protecting both the robot and the NDE sensors from damage due to the pipe environment, moisture, corrosive agents (if any), etc.,
- The interference of other substance presence in the pipe during inspection, e.g., presence of water droplets, moisture, etc.,

- Heat dissipation control and fire prevention, and
- Additional robot construct/modification necessary to accommodate NDE sensor unit's, e.g., circumferential scanning and vice versa.

TASK 2.4: INITIAL NDE SENSOR SYSTEM SPECIFICATIONS

Based on the outcome of Tasks 2.1-2.3 above, a set of initial specification for the NDE sensors were created as shown in **Table 4**. Note that some parts of the specification are for robot development as they affect the specifications of the sensors the robot is to carry. On the NDE sensor side, these specifications address directly or indirectly the following areas of concern:

- Minimum “detectability” capability of the NDE sensor(s) systems,
- Physical size limitation for the NDE sensor unit specifically (per given pipe diameter size),
- Influence of soil properties (i.e., backfill) outside the pipe,
- Power supply requirements (e.g., battery capability) for the NDE sensor unit,
- On-board data storage capability, and data processing and transfer requirements,
- Requirements for speed and precision for the NDE sensor(s) system’s movement (along pipe axial direction),
- Scan speed, precision, and stability requirements for the NDE sensor(s) system,
- Additional specifications with the robot unit,
- Evaluation criteria for NDE sensor(s) system performance, e.g., scan speed, critical flaw size, etc.
- Evaluation of probe/array density -vs- scan paths (such as helical, axial, etc.) on scan speed and system cost.

Note that this set of initial specification for the NDE system(s) were put in place for the subsequent feasibility and design studies to be conducted under Tasks 2.7 -2.9 as described below, and are subject to update and change during the project. For example, the pipe diameter as small as 2” was shown in the specification as “must have”. However, it appears that 4” - 6” diameter is most likely the limit that current technology can achieve. In addition, a few critical parameters remain undetermined and thus, are not included in the specification. Two of them are inspection resolution and critical flaw size, both requiring further input/data from the field.

Table 4. The initial specifications for both NDE sensors and robot modules.

color code:		
MUST HAVE	GOOD TO HAVE	NOT IMPORTANT
SYSTEM CHARACTERISTICS		IMPORTANCE
Pipe Material	HDPE	
	MDPE	
Pipe Diameter	1"	
	2"	
	4"	
	6"	
	8"	
Operating Pressure	60psi	
	124 psi	
Live Launching and Retrieval	Vertical Saddle	
	Angled Saddle	
Live inspection		
Obstacles Negotiation	Vertical Segments	
	Inclined Segments	
	Bends	
	Tees	
	Reducers	
	Fusion joints	
	Valves	
Bi-Directional Operation		
Tetherless		
Live Control of Robot		
Range of Robot	500 ft	
	1,000 ft	
	2,500 ft	
	5,000 ft	
Inspection speed	500 ft/hr (2"/s)	
	1,000 ft/hr (4"/s)	
	2,500 ft/hr (10"/s)	
Video camera	Live Feed	
	Recorded images	
Defect Detection	Delamination	
	Foreign objects in material/joints	
	Gouges/Mechanical Damage	
	Cracks	
	Cold Butt Fusion	
	Defective electrofusion	

TASK 2.5: TECHNOLOGY REVIEW – NDE SENSOR TECHNIQUES

In Task 2.35 we performed a limited literature search, pertinent to the objectives of this particular inspection challenge and as it relates to NDE methods that are already in use or have demonstrated real promise for utility. This technology review was conducted in the June-July 2021 period. The outcome of this task is detailed in Appendix 1, and is in the form of a “trade-off table” outlining each method’s advantages and limitations. This effort concentrated on inspection-related issues and not those related to how the methods may be incorporated into a robot, etc. The following techniques were rejected (primary reason as shown):

- Eddy current – only work in electrically conductive media
- X-ray – equipment size too large to fit into interior of the pipe
- Shearography – not applicable to project’s small diameter pipes
- Thermography – penetration depth is limited
- Magnetic particle – only work with ferromagnetic materials
- Electromagnetic acoustic transducer – only work in electrically conductive media

After a thorough review against all other possible NDE techniques currently available, the three techniques as originally proposed, namely, air-coupled ultrasonics (UT), microwave/millimeter wave imaging (MW/MMW) and terahertz imaging (THz), remain the leading and favorable candidates.

TASK 2.6: MILESTONE MEETING FOR TECHNOLOGY REVIEW

An interim milestone meeting took place in October 2021 to review all project activities up to that point, including Tasks 2.2 -2.5 and initial design and experimental work of Tasks 2.7 – 2.9. The primary outcome was to determine which NDE technique(s) should continue to be considered for further development. A similar effort was carried out to review the robot technology. The report generated from Tasks 2.4 and 2.5 above, along with the robot technology review results were presented to the funders at this meeting.

Prior to the milestone meeting, a series of online discussions occurred during June-September on detection priority of SWG naturally occurring defects. It was revealed that SWG defects fall generally into three categories:

- *Internal degradation*: degradation mechanism (some originated from subsurface voids) causes delamination leading to blistering, peeling and cracking on pipe's inner surface; highest risk,
- *Contamination*: foreign materials such as nylon and polyester causes delamination and cracking; medium risk
- *External degradation*: degradation mechanism (some originated from subsurface voids) causes delamination leading to blistering and peeling on pipe's outer surface; low risk

Figure 7 shows these three types of SWG defects. These defects were given different priorities of repair depending on the locations and severity. For example, external degradation that equals or exceeds 10% of the wall thickness of the pipe are scheduled for replacement. The root causes of internal and external degradation are considered separate and independent. The importance of defect location and types related to SWG needs were stressed in the discussions. Separately, ISU team brought in the concepts of probability of detection (POD) and false alarm (PFA) and showed how they affect detectability. It was generally understood that currently there are no sufficient field data and experience to support these POD and PFA activities. ISU team then introduced the model-assisted POD (MAPOD) approach in which the use of model simulation can help leveraging the limited experimental testing being conducted. These SWG discussions were presented in the milestone meeting.

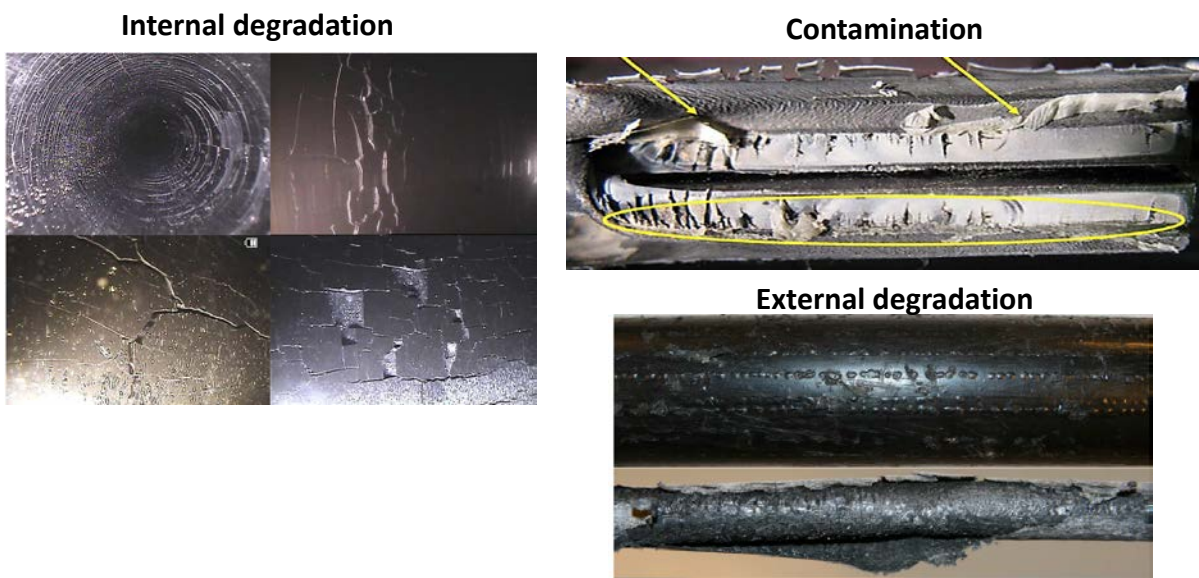


Figure 7: The SWG defects: internal and external degradations and contamination

The following general recommendations were given for the three NDE techniques:

- Microwave – Consistent with our initial expectations, microwave methods have potential for detecting certain flaws in 4” pipe or larger. Microwave testing allows for fast scan speed. Drawbacks is the limited range resolution, which provide limited depth information,
- Ultrasonics – Pipes as small as 4”, medium scan speeds, good depth sensitivity, modes and beam arrangements available to optimize sensitivity to all flaw types,
- Terahertz – Pipes as small as 6” (4” may be possible), good detection, depth sensitivities and potential of defect identification; array approach for faster scan speed viable.

Following this milestone meeting, the funders approved the recommendation presented for the NDE technologies with a *Proceed with all three techniques for further evaluation*. The NDE sensor specifications were revised based on the work done to this point.

In the milestone meeting, it was also announced that a samples inventory containing 12 samples was available to the project. This set included pipe samples with engineered (machined) defects and pipe samples with naturally occurring defects that were cut/sections to facilitate inspections using laboratory equipment. Examples of naturally occurring and engineered defects are shown in **Figure 8**.

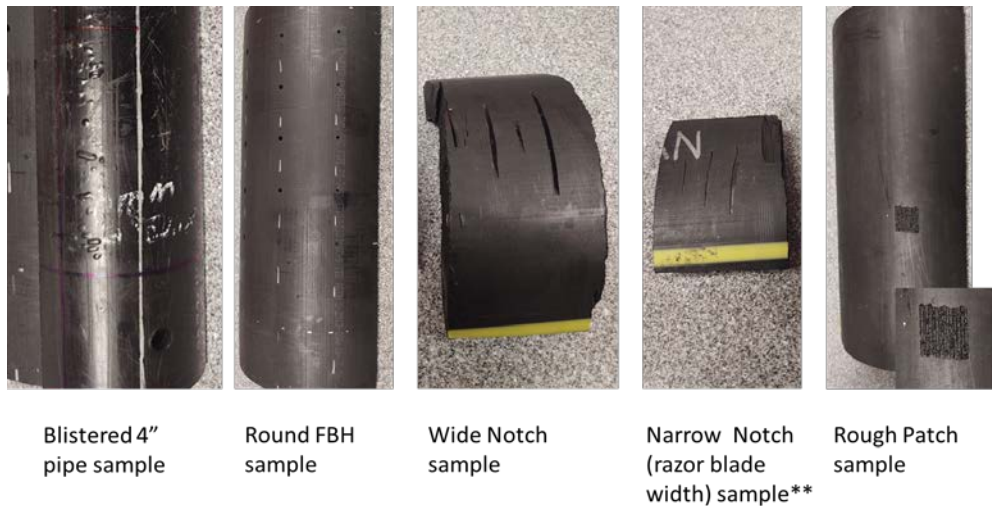


Figure 8: Examples of sample inventory containing naturally occurring and engineering defects.

TASK 2.7: FEASIBILITY AND DESIGN STUDY – THZ IMAGING AND SPECTROSCOPY

In this section, we describe in details the development and conceptual design of a THz sensor. The main efforts were made in experimental testing, model simulation, and conceptual design of the miniaturized sensor modules. Details on the technique can be found in Appendix 1: Report on Technology Review – NDE Sensor Techniques below.

Task 2.7.1 Miniaturization Challenges

In this project, we are tasked to construct a THz imaging system for inspecting plastic pipes from the inside. As the specification requirements pushed for smaller and smaller pipe diameter, resulting in smaller and smaller allowable space for the system, this task became quite challenging. Fortunately, the challenges lie in the engineering for miniaturizing existing THz components and not in the science for discovering new way of generating a THz source for this application. The key issue is that the components of the THz system need to fit into multiple linked robotic modules, which in turn are required to fit inside of plastic pipes of 4-inch and 6-inch diameter. The other major issue was to fine tune the sensor setup for optimal inspection for which we employed model simulations in place of time-consuming and cost-ineffective experimental studies (see Task 2.7.3 below).

To overcome these challenges, we have taken the following steps:

- a. Performed initial screening to determine the optimal approach in meeting the objectives. The approaches to be considered include photoconductive antenna, optical rectification, and integrated circuit,
- b. Based on the approach choice from Task (a), determine the minimum sets of components required for the THz system, e.g., laser, laser controller, THz transmitter, THz receiver, lenses, delay lines, chopper, analog-to-digital converter, mini-computer, data storage. Batteries are excluded,
- c. Based on the hardware components currently available in the photonic market (Task 2.7.4 below), perform miniaturization of each system components determined in Step (b) to see if all system components can fit into multiple linked robotic modules which in turn are required to fit inside of plastic pipes of 4-inch and 6-inch diameter, respectively,

- d. If Step (c) is feasible, consider extending the system to array of 4 or 6 transmitter-receiver pairs (each pair covering 60° or 90° aperture of the pipe cross section) by using more space of the linked robotic modules,
- e. Determine the placement of all system components of the system in the linked robotic modules for Steps (c) and (d),
- f. Fine tune the system components to meet the performance specs such as temporal data length, resolutions and signal-to-noise ratios (via focusing lens, etc.) for detecting critical defect size within the pipe wall and carrying the inspection at the desired speed,
- g. Construct the draft CAD model design of the system based on outcomes from Steps (c) – (f),
- h. Provide estimations of additional specs such as electric power consumption and overall weight and dimensions of the system.

From what we learned about the photonic products in current market, constructing a miniaturized THz inspection system for 4” pipe diameter is within reach. Given the limited budget, however, the work described here represents the best efforts possible in this current phase of the project in determining the feasibility of the approach, in estimating the fitness of the system components and other specs to the pipe sizes, and in designing the draft CAD models. More detailed and thorough work will be needed using new hardware available at the time that the actual prototype system will be built in a future phase of the project given the rapid technological developments in this field.

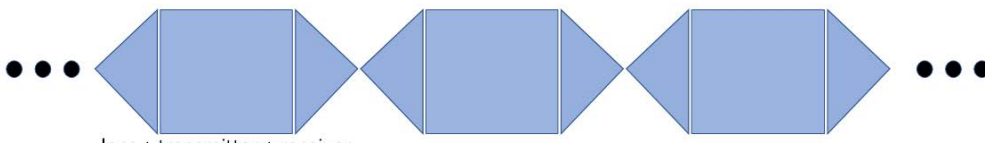


Figure 9: Conceptual illustration of a THz miniaturized system mounted in a 3-module robot train.

Task 2.7.2: Property and Benchmark Measurements

Extensive experimental testing was carried out on the set of engineering and naturally occurring samples made for this project (as described above). The testing was conducted by using ISU-CNDE's pulsed THz imaging system which has exceptional longitudinal (in time or equivalently in distance) and lateral spatial resolutions. This pulsed THz imaging system was manufactured by TeraView Ltd. based in Cambridge, United Kingdom (<https://teraview.com/>). The THz pulse generation employs the popular photoconductive antenna approach, and offers a wide spectrum from 50GHz to 4THz at 5GHz data resolution using a patterned "resistor on a chip" technology. The gantry of the imaging system allows two-axis scan in both planar and rotary modes. **Figure 10** shows both types of scans: two linear translation drives are used for planar mode and one linear drive pairs with a turntable for rotary mode.

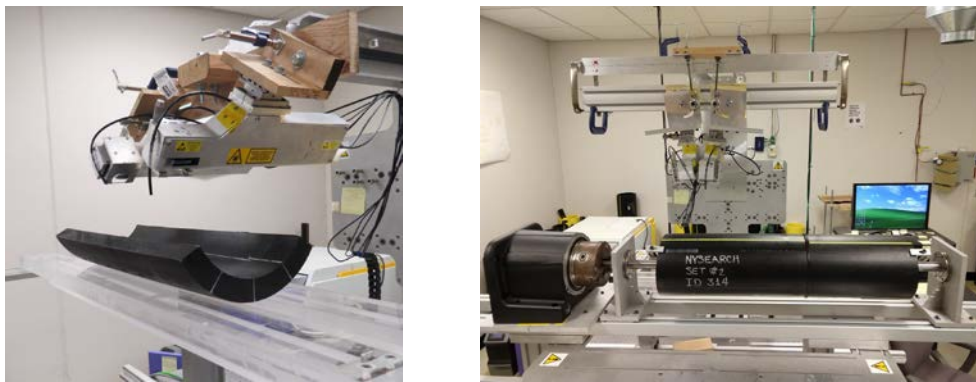


Figure 10: ISU-CNDE's pulsed THz imaging system performs two-axis planar mode (left) and rotary mode (right) scans on pipe sample from the inner surface outwards.

The transmitter-receiver pair was configured to acquire one-sided reflection measurements. For pipe testing, the planar mode scan was only used for scanning narrow areas or small-size samples made from large diameter pipe in which cases the local curvature in the scan area may be sufficient large for the area to be scanned in planar mode. In the following, all scans were carried out from the pipe's inner surface outwards as if the pipe was inspected from the inside during an in-line inspection. Volumetric A-scan data were acquired for all scans and were further processed by in-house software to produce B-, and C-scan images or additional forms of data representations. The A-, B- and C-scan data representations, similar to that used in ultrasonics, are well known in

FOR PUBLIC RELEASE

the literature (e.g., <https://www.nde-ed.org/>).

Figure 11 shows the two views of sample #1 which has three rows of 5 flat bottom holes (FBHs) of diameters 1/8", 3/16" and 1/4" drilled from pipe's outer surface at 5 different depths. Examples of A-scan waveforms and C-scan images are plotted in **Figs. 12 and 13** for 1/8" hole row and 1/4" hole row, respectively. Since the FBHs are at different depths, by gating specific time to match a specific depth we are able to detect the corresponding FBH at that depth. For the 1/4" FBH, the hole footprint stands above the background strongly owing to its larger reflecting surface. For the smaller 1/8" FBH, the hole footprint can still be identified clearly but with lower signal-to-noise ratio against the background.

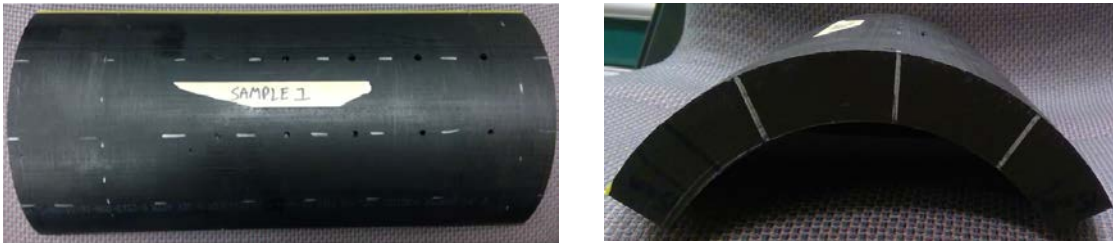


Figure 11: Two views of sample #1.

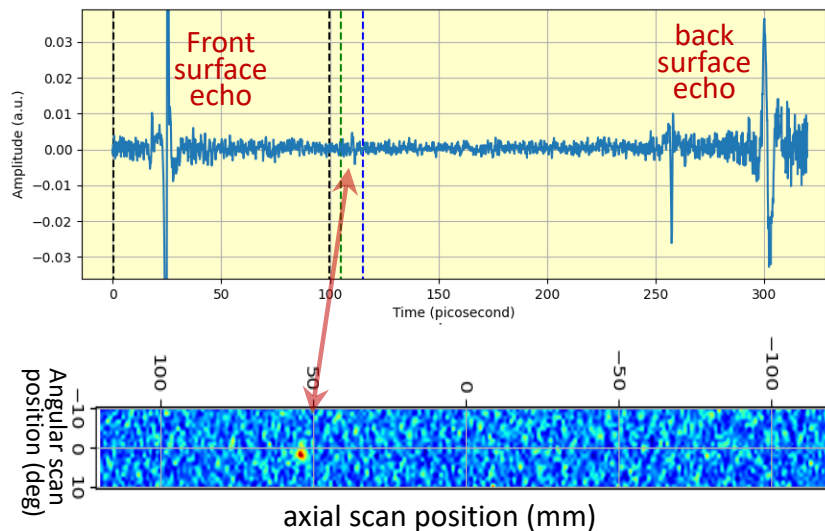


Figure 12: Examples of A- and C-scans for a 1/8" flat-bottom hole in sample #1.

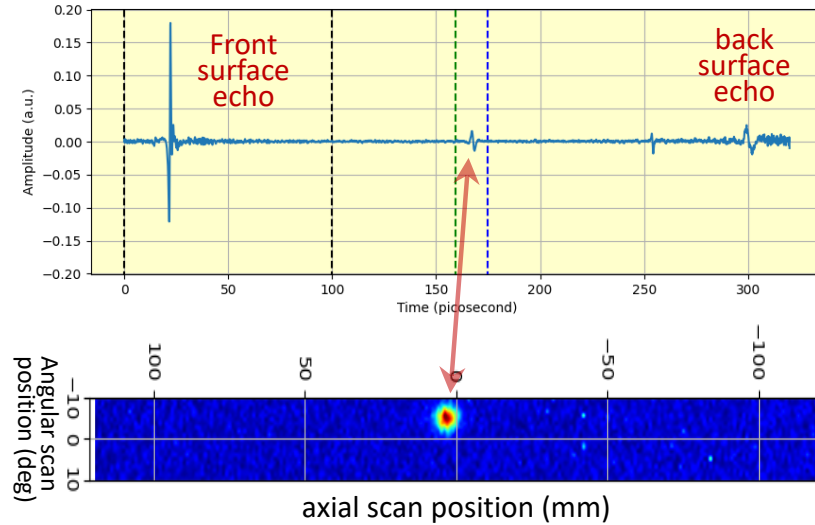


Figure 13: Examples of A- and C-scans of a 1/4" flat-bottom hole in sample #1.

As shown in **Figure 14**, sample #2 contains different types of synthetic defects: three slot cuts on left and one square roughened area on right (as enclosed), all made on the outer surface of the pipe. The THz scan was able to detect both types of defects.



Figure 14: Three slot cuts (left) and one square roughened area (right as enclosed) made on sample #2.

Next, we present scan results of sample #3. Similar to sample #1, this sample also has three rows of five FBHs at different depths, except that the FBH diameters are larger. B and C-Scans show all five holes (**Figure 15**).

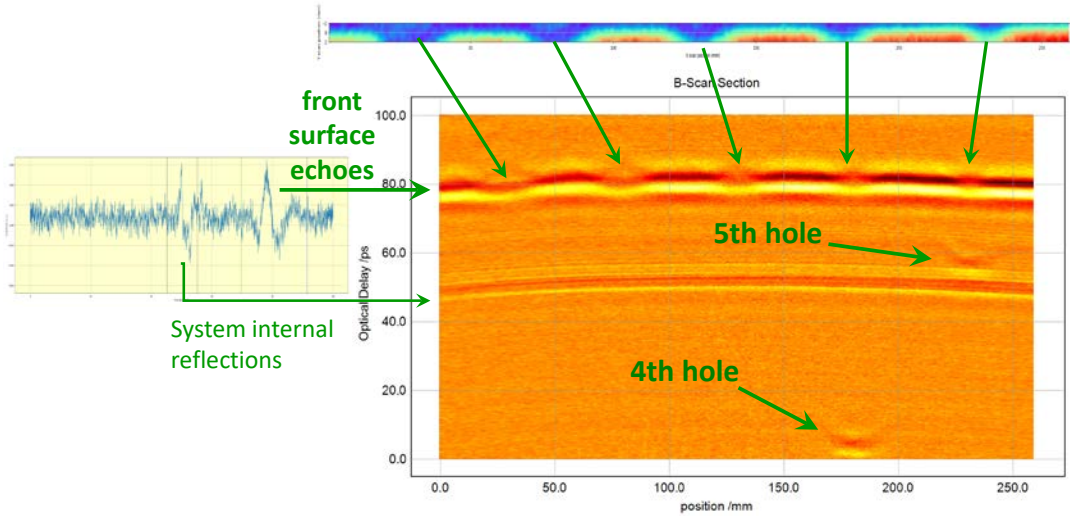


Figure 15: . B- and C-scans show all five 3/8” FBHs in Sample #3.

Sample #4 has small size but is packed with three shallow FBHs and two taped squares (**Figure 16**). The FBH sizes are 1/8”, 1/4” and 3/8”. One taped square has one-layer duct tape and the other has two layers of duct tape glue-to-glue to create air gap between the tape and pipe’s front surface. **Figure 18** plots A- and B-scan where the three FBHs are clearly visible.

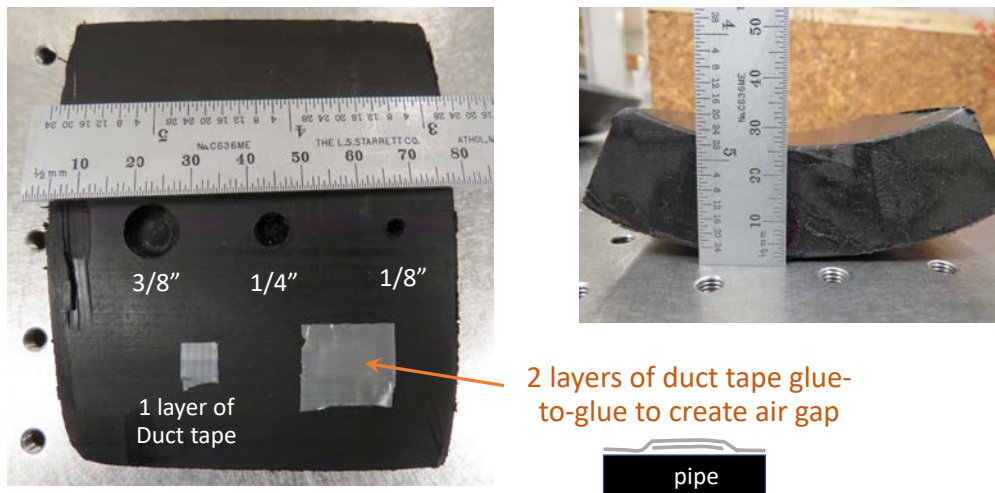


Figure 15: Sample #4 has three shallow FBHs and two taped squares.



Figure 17: Planar scan performed on sample #4.

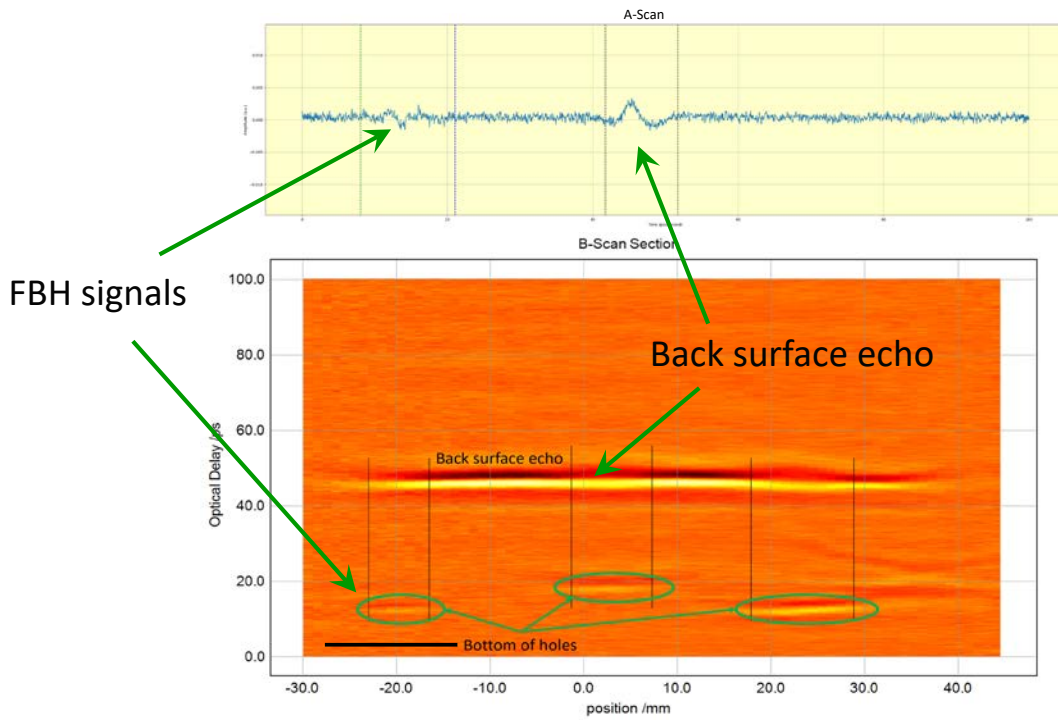


Figure 18: A-and B-scan identify the three FBHs on sample #4.

Sample #6 with three shallow slot cuts is particularly small in size. Its small size posted some difficulty in setting up the scan. We managed to resolve this difficulty by using sample #5 to pivot the rotation of sample #6 in scan (**Figure 19**). The three slot cuts were detected with lower amplitude than background in C-scan (**Figure 20**). The bottom slot was, however, shadowed by the very strong amplitude of the nearby aluminum tape marker.

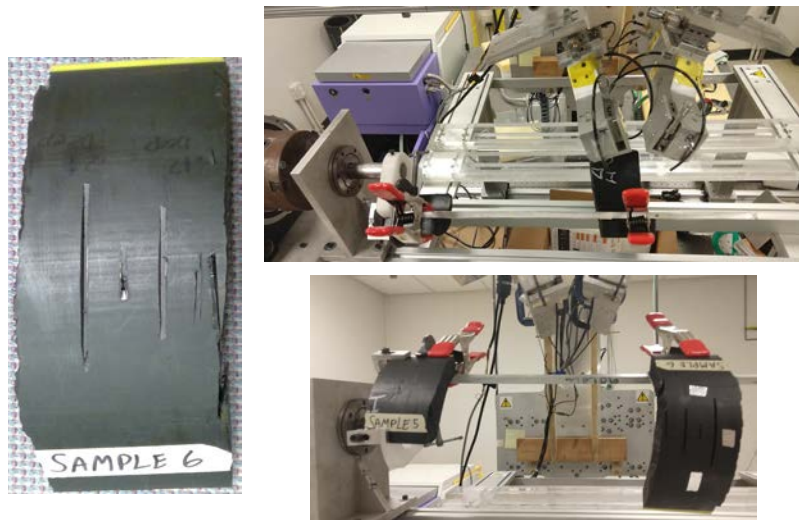


Figure 19: Sample #6 (left) and the experimental setup (right).

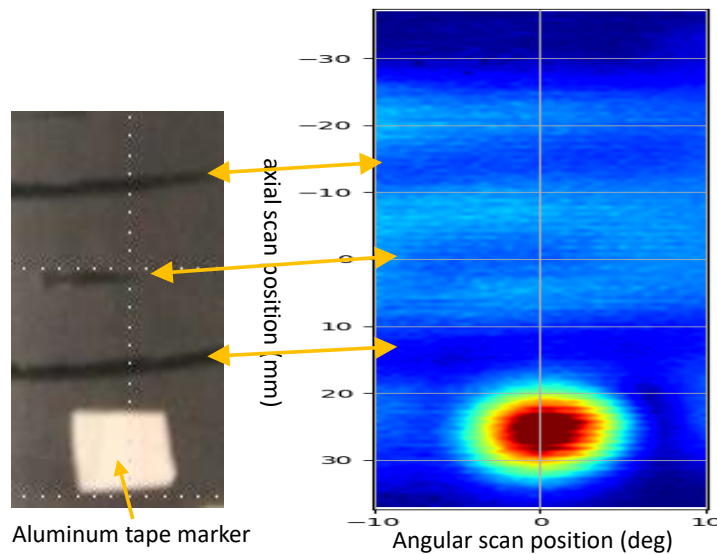


Figure 20: The three slots on sample #6 (left) with low-amplitude on C-scan (right). Bottom slot shadowed by nearby aluminum tape marker.

Samples 8-10 were cut evenly one third each from a SWG field pipe section having total external degradation as described in Section 2.6 and seen in Figure 7. This external degradation appears as high-density blisters or “bubbles” formed on the pipe’s outer surface. **Figure 21** depicts the formation of the blisters on sample #8 in more details. We have performed rotational scan on sample #8 (**Figure 22**). As shown in **Figure 23**, we are able to image the bubbles in high definition. However, the bubbles’ C-scan images were overpowered by the strong reflections from the surrounding aluminum tape markers and shown with low amplitude. This can be improved, as shown in **Figure 24**, by fine tuning the system.

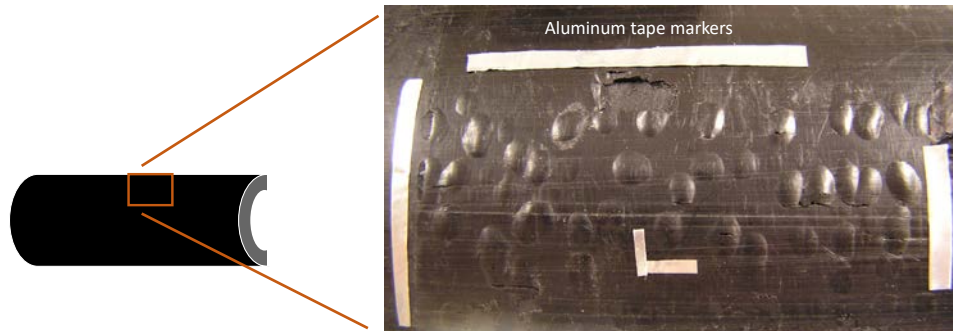


Figure 21: External degradation in the form of high-density blisters on sample #8.

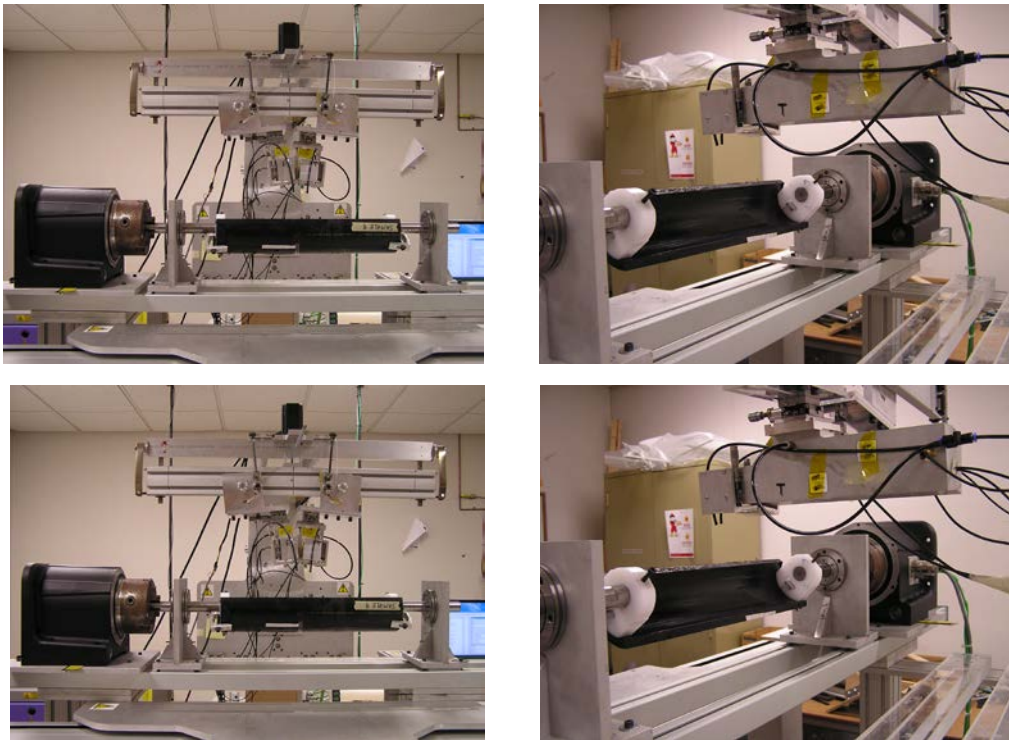


Figure 22: THz rotational scan performed on sample #8.

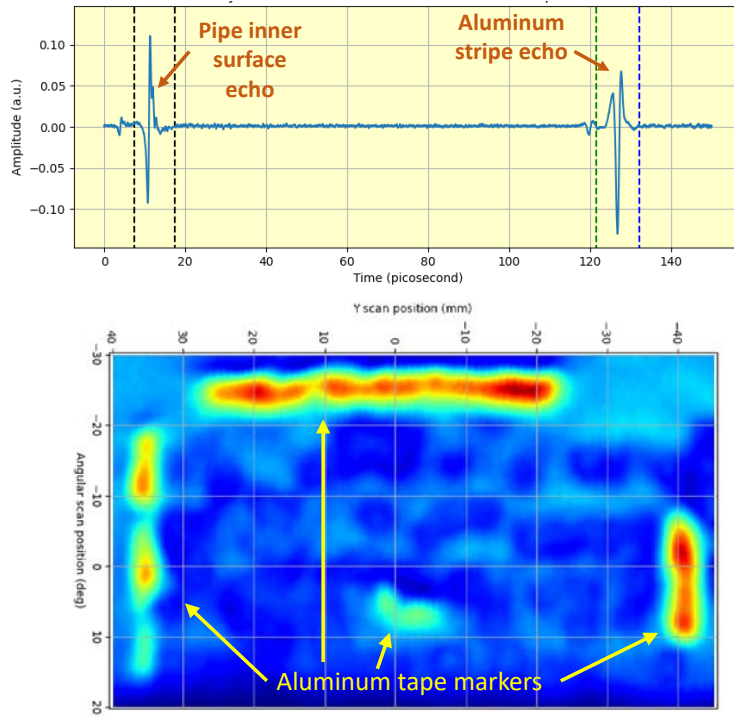


Figure 23: A- and C-scan results on sample #8 by time gating at the front surface echoes.

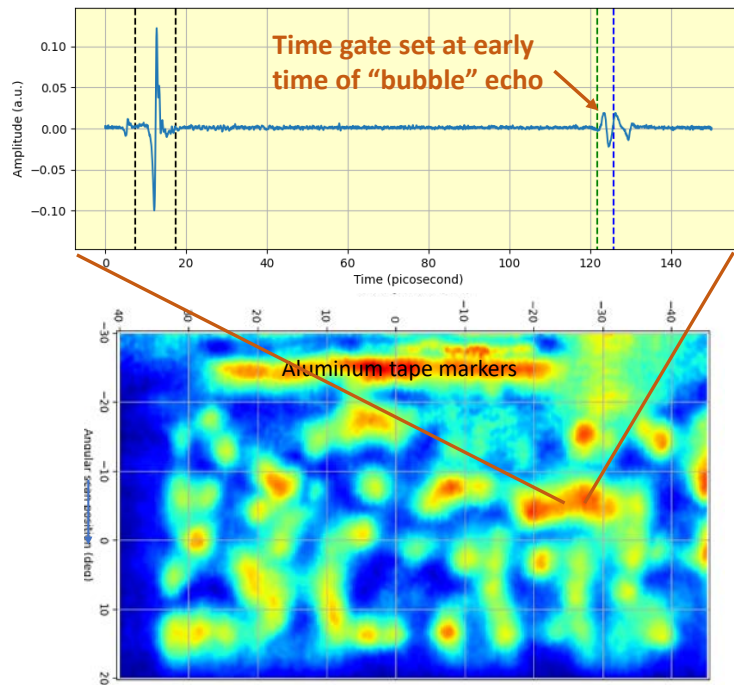


Figure 24: A- and C-scan results on sample #8 by gating at early time of "bubble" echoes.

We then proceeded to simulate the actual environment underground outside the pipe by backfilling a soil patch and taped it onto the same scan area and rescan again with the same settings (**Figure 25**). The rescan results are shown in **Figure 26**, which has essentially preserved all the main feature with little loss. This would be the most important result for THz technique in all experimental testing in this project: *THz time-domain pulsed system possesses high temporal resolutions and hence great depth sensitivity. With this capability, the environment outside the pipe such as backfill soil has little effect to THz detection and differentiation of pipe's outer surface delamination, i.e., the "bubbles".*

Given the success gained in the scanning of sample #8, we expect to see similar results from samples # 9 and #10 (which, as previously noted, are the other two one-thirds of the same pipe section). To demonstrate this, here we furnish scan results of smaller scale for each sample in **Figs. 27 and 28**, respectively.

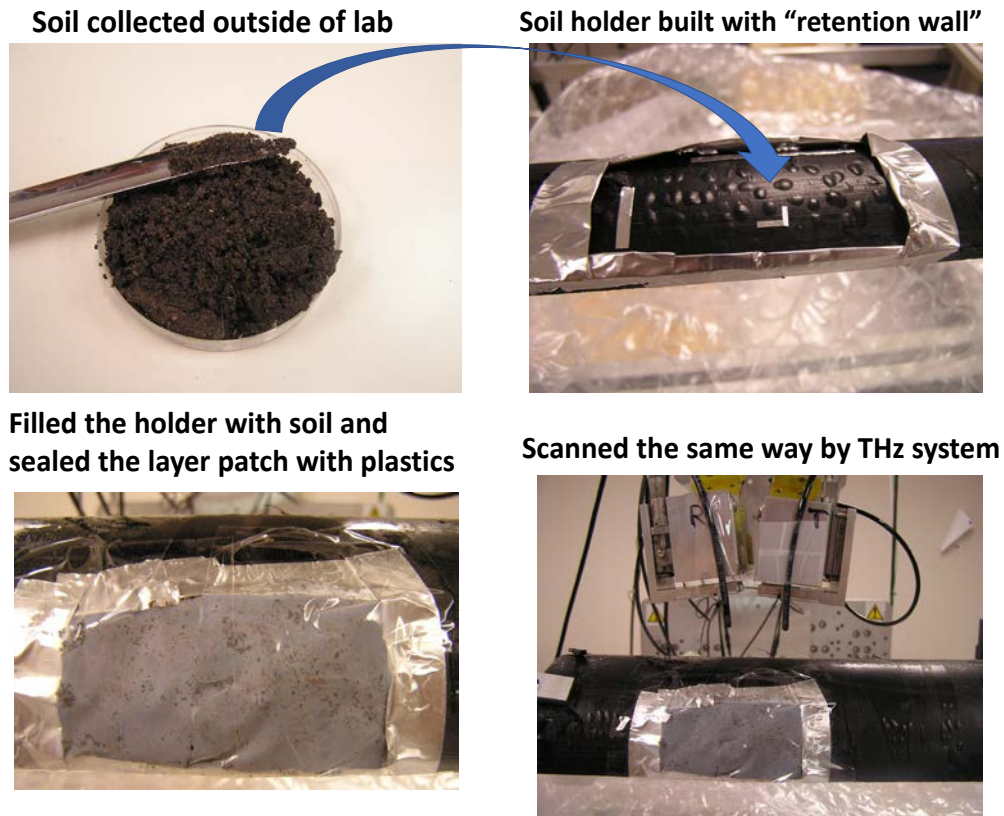


Figure 25: Simulating field environment by attaching a backfill soil patch to pipe surface (top) and rescan (bottom).

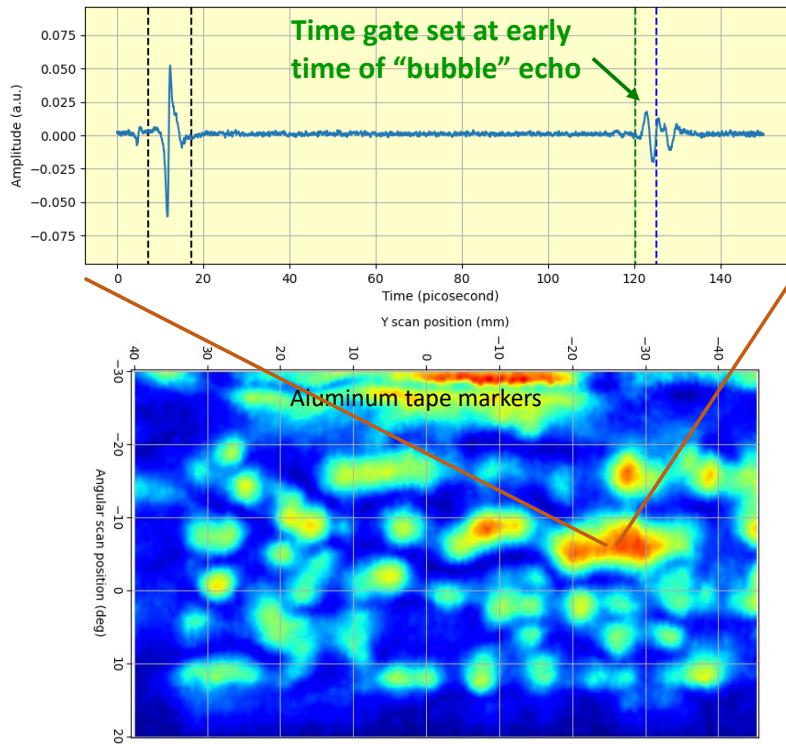


Figure 26: A- and C-scan results on sample #8 by time gating at early “bubble” signal with simulated backfill soil attached.

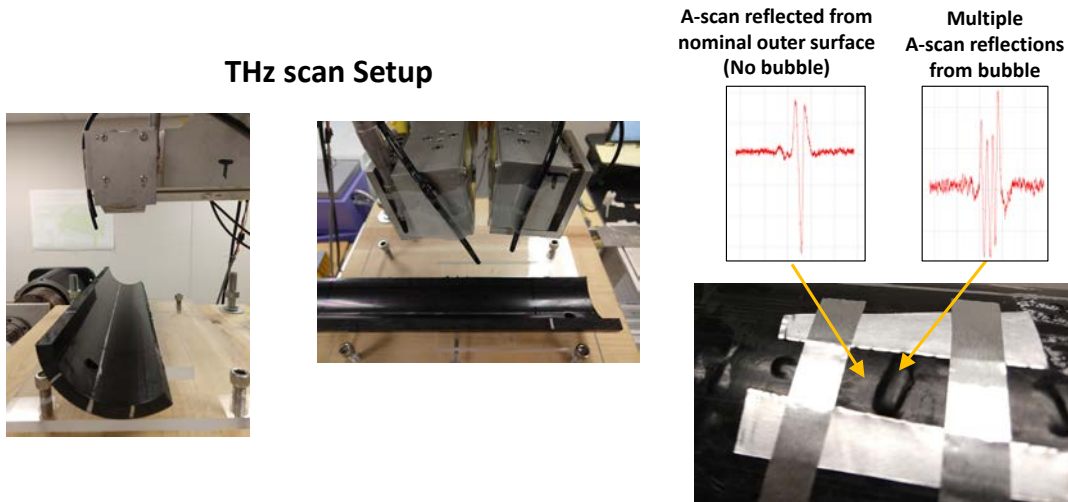


Figure 27: Setup and C-scan results for sample #9.

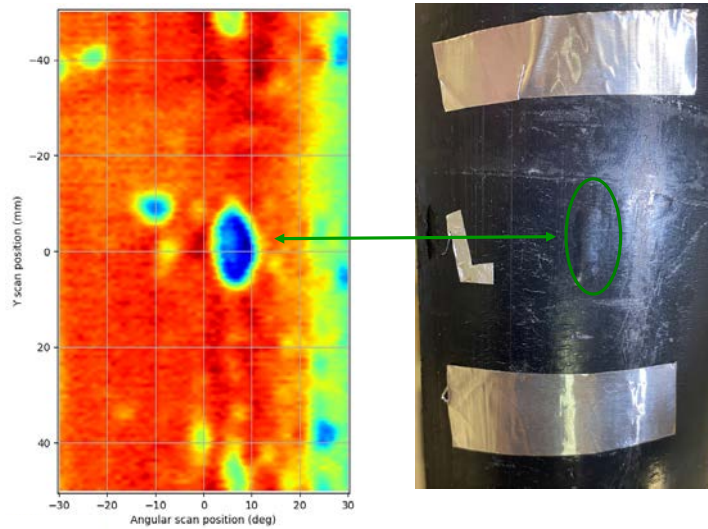


Figure 28: C-scan results for sample #10.

Task 2.7.3 Design Optimization by Simulation

Anticipating limited experimental work to be allocated in this initial phase, a portion of the feasibility study was carried out computationally. For this, a first-generation ray-tracing based THz inspection simulator was developed at CNDE, which is particularly useful for optimizing the THz sensor setup with minimum turnaround time. In this first-generation THz simulator, we captured the basic ray-tracing concepts and algorithms based on principles of optics. The parameters to be examined by simulation include:

- Transmitter and receiver placement and orientation,
- Operating frequency range, and
- Lens design for optimal focusing.

The ray-tracing model and its visual aids allow us to perform a virtual inspection from inside of the pipe as was in the actual experimental testing. The inspection settings simulated were: 4” pipe; ¼” lens diameter; 30mm focal length; 70⁰ T-R separation angle. The settings were corrected/optimized after the initial results were reviewed, and as a result the focus and reception at the receiver were greatly improved.

As illustrated above, this THz simulator, although still at early stage of development, has captured the essences of a THz inspection process and provided a good visual aid of the ray interaction with the part. We intend to continue developing this ray-tracing simulator in the future phases of the project to allow direct comparison with the experimental data in terms of the A-and C-scans.

Task 2.7.4 Hardware Availability - Market Survey

To be able to realistically design the miniaturized THz inspection system, we surveyed the current THz market. The availability of the most cost-effective components for constructing the THz sensor unit was also assessed.

The laser appears to be the critical component for size consideration. Shown in **Figure 29** is a miniaturized erbium-doped femtosecond fiber laser head made by IMRA (model AX-20; <https://www.imra.com/>). At a very small footprint, this laser is still capable of delivering pulse less than 100 fs long with 25mW output power and at 50 MHz repetition rate. After disassembling, its components are likely to be able to be re-packed and fit into 4” pipe’s cylindrical space. The same applies to the laser’s controller. In fact, these laser components had been successfully utilized in manufacturing a handheld THz spectrometer Micro-Z ([3], **Figure 30**), one of the earliest miniaturized THz commercial systems.



Figure 29: A miniaturized erbium-doped femtosecond fiber laser head

Another notable engineering design along this line was a rotary involute delay stage (**Figure 31**).

Its four-wing design improves waveform acquisition rate to 550Hz while delivering 115 ps delay range [3].



Figure 30: Micro-Z: a handheld spectrometer as one of earliest miniaturized THz system [3].

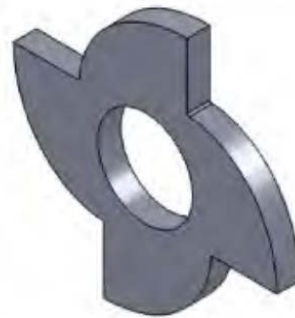


Figure 31: A 4-wing rotary involute delay stage for fast data acquisition rate [3].

Task 2.7.5 Enhancement by Post-Processing

The THz data collected from long-distance pipe inspection are massive and often corrupted by background noise. In this project, signal and image processing were constantly utilized to smooth the data and/or clean out unwanted interference or background noise. Advanced analysis tool such as contour following or front surface echo following was also applied to the data beyond the nominal A-, B-, and C-scan presentations. In fact, most of the THz results shown in Section 2.7 had been post processed by some of these techniques using our own in-house software. The contour following technique was well developed and widely used in NDE industry, e.g., <https://www.tecscan.ca/automated-contour-following-for-ndt-ultrasonic-testing-of-large-aerospace-parts/>.

Advanced detection enhancing algorithm such as SAFT and machine learning related methods should be implemented in future phases.

TASK 2.8: FEASIBILITY AND DESIGN STUDY – MICROWAVE WAVE IMAGING

From [4] microwave imaging is described as the following: “Microwave and millimeter-wave imaging is the process of creating a 2D (or 3D) map of electromagnetic properties of an Multi Unit Testbed (MUT). The electromagnetic property can be an intrinsic material property, such as relative complex permittivity (ϵ_r) or relative permeability (μ_r), or can be quantities that are proportional to these material properties such as reflectivity as well as geometrical features (e.g., a crack). Therefore, such images are produced as a function of material property contrast in an object and geometry (relative to the operating wavelength). Microwave imaging probes are essentially antennas. Hence, imaging techniques can primarily be classified as either near-field or far-field techniques depending on the (electrical) distance between the probe and the MUT. Microwave images are primarily produced using raster scanning, although in lieu of mechanical (raster) scanning, 1D and 2D arrays of antennas can be assembled, to perform rapid electronic scanning. In either case a 2D matrix consisting of measured data, commonly a DC voltage or complex scattering parameters, as a function of frequency and proportional to the local reflection properties in a specimen is obtained. The collected data is then mapped directly to a contrast image or processed using backpropagation algorithms (e.g., SAR). Thus, the choice of imaging technique, probe type, and frequency of operation are dependent on the sample properties and the target features (e.g., crack, void, delamination, etc.)”

With respect to synthetic aperture radar (SAR) imaging, also from [4]: “High-resolution imaging methods, based on (backpropagation) SAR algorithms, are capable of producing three-dimensional (3D) holographic images of dielectric structures. Such imaging methods are extremely valuable for inspecting the ever-increasingly utilized nonconductive composite structures that have been replacing metals in many industries. A small antenna (with broad radiation pattern) is raster scanned along a one-dimensional (1D) path or across a two-dimensional (2D) grid forming a synthetic array or aperture. The antenna is connected to a wideband reflectometer which performs coherent (referenced) reflection measurements from multiple angles (views) of the sample. The collected reflected data is then processed by a fast 3D SAR algorithm (e.g., ω -k algorithm) to produce a 2D or 3D holographic image of the sample under test. The cross-range resolution is on the order of $\frac{\lambda}{4}$ at distance close to the synthetic array and it degrades (becomes

aperture limited) as distance increases. 3D imaging can also be performed in non-Cartesian planes (e.g., cylindrical) using the appropriate algorithms such as SAR or time reversal.”

Task 2.8.1: Design Optimization by Simulation

The first step in this investigation involved using electromagnetic (EM) simulations to gain an understating of capabilities and limitations of microwave NDT for inspecting defects such as delamination (special case of an internal void, but more challenging to detect than a void) within an HDPE pipe. Consequently, simulations were performed using CST Studio Suite®, a commercial numerical EM modeling software, to study the efficacy of microwave NDT for inspecting HDPE pipes. The simulations were conducted for a section of a 6” pipe containing with a wall thickness of 1” containing a disk-shaped delamination of diameters in the range of 9 mm to 19 mm and depth in the range of 2 mm to 8 mm, as illustrated in **Figure 32**. As illustrated, a sensor consisting of a K-band (18-26.5 GHz) open-ended waveguide probe was scanned circumferentially away from the center of the delamination. This waveguide band and the operating frequency range was chosen since it includes the 24 GHz industrial, scientific, and medical (ISM) band [5-6]. At this band, there is a significant availability of commercial off-the-shelf microwave components and radar system on-chip integrated circuits (ICs) that can be used for constructing small sensors. Reflection

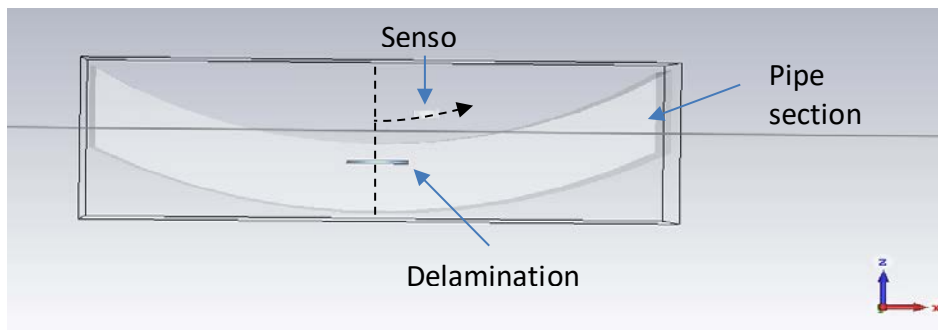


Figure 32: CST Studio Suite® simulation model for detecting delamination in HDPE pipes using an open-ended waveguide probe.

coefficient (S_{11}), which is a ratio of reflected electric field to transmitted electric field, simulations were performed for “delaminations” with varying diameters and depths (distance from inner wall). Reflection coefficient changes as a function of material properties, dimensions of a part, presence of flaws (discontinuities), etc. **Figure 33** shows a set of these simulated reflection coefficients (S_{11}) in the complex (real-imaginary) plane for a “delamination” with a diameter of 19 mm and a depth of 6.12 mm. The results show that the change in reflection coefficient is quite measurably significant when the sensor is scanned across the delamination. **Figure 34** shows the simulated magnitude of reflection coefficient, $|S_{11}|$, at 24 GHz for three “delaminations” with diameters of 9, 13, and 19 mm and a depth of 6.12 mm, as a function of sensor lateral distance from “delamination”

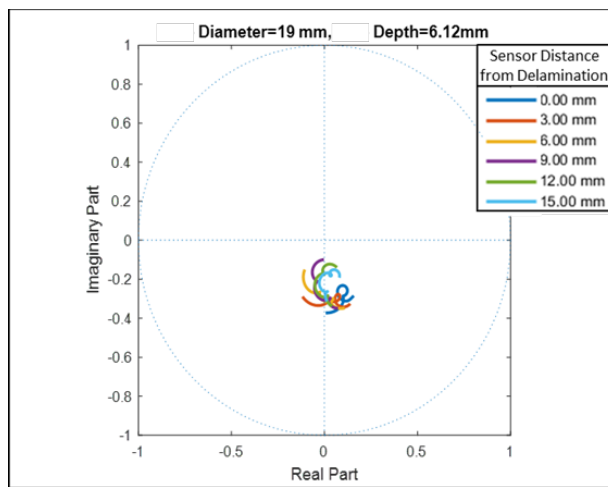


Figure 33: Simulated reflection coefficient (S_{11}) for a delamination with a diameter of 19 mm and a depth of 6.12 mm, shown in the complex (real-imaginary) plane. The reflection coefficients change clockwise as frequency increases from 18 to 26.5 GHz.

center. As shown, the sensor produces a significant change (0.170 to 0.305) when scanned over the larger (19 mm) delamination. Note that the range of $|S_{11}|$ is 0 to 1, therefore this change represents a 13.5% change. On the other hand, the results show no change in $|S_{11}|$ for the two smaller “delaminations” at the frequency of 24 GHz. This is likely due to the combination of thickness of pipe wall and distance of sensor to the pipe walls, as well as the location of the delamination as a function of wavelength (frequency), which causes signal interference in such a way that response from the delamination is weak, such as when the delamination depth is equivalent to quarter-wavelength in the pipe material. **Figure 35** shows similar results for

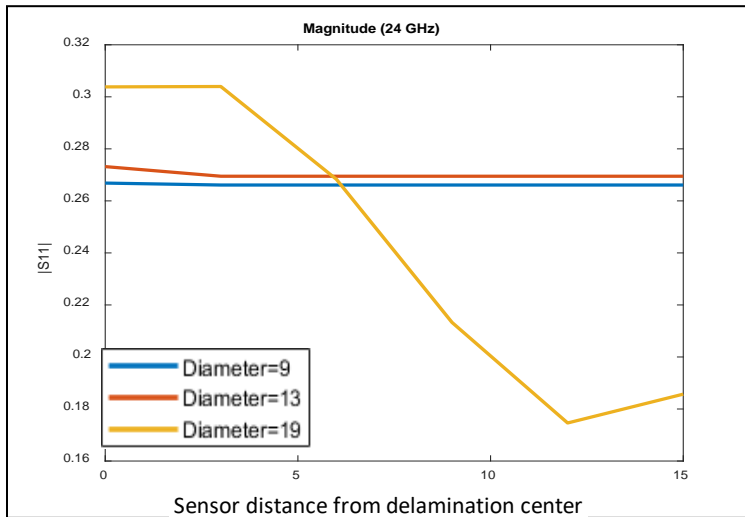


Figure 34: Simulated magnitude of reflection coefficient (S_{11}), at an operating frequency of 24 GHz, for three delaminations with diameters of 9, 13, and 19 mm and a depth of 6.12 mm, as a function of sensor distance from the delamination center.

delamination placed at depths of 2 mm, 3 mm and 5 mm, respectively. As shown, operating at 24 GHz, the microwave probe is sensitive to the presence of “delamination” at various depths within the pipe wall. For the specific case of the 6.12 mm depth, slight changes in frequency will result in moving the interference pattern sufficiently to detect these “delaminations”, as will be shown experimentally in the next section. This indicates the need for using a sensor with some frequency bandwidth by which this interference may be averaged out. As will be shown later experimentally, using a range of frequencies along with SAR processing allows for improving the signal to noise ratio of an image.

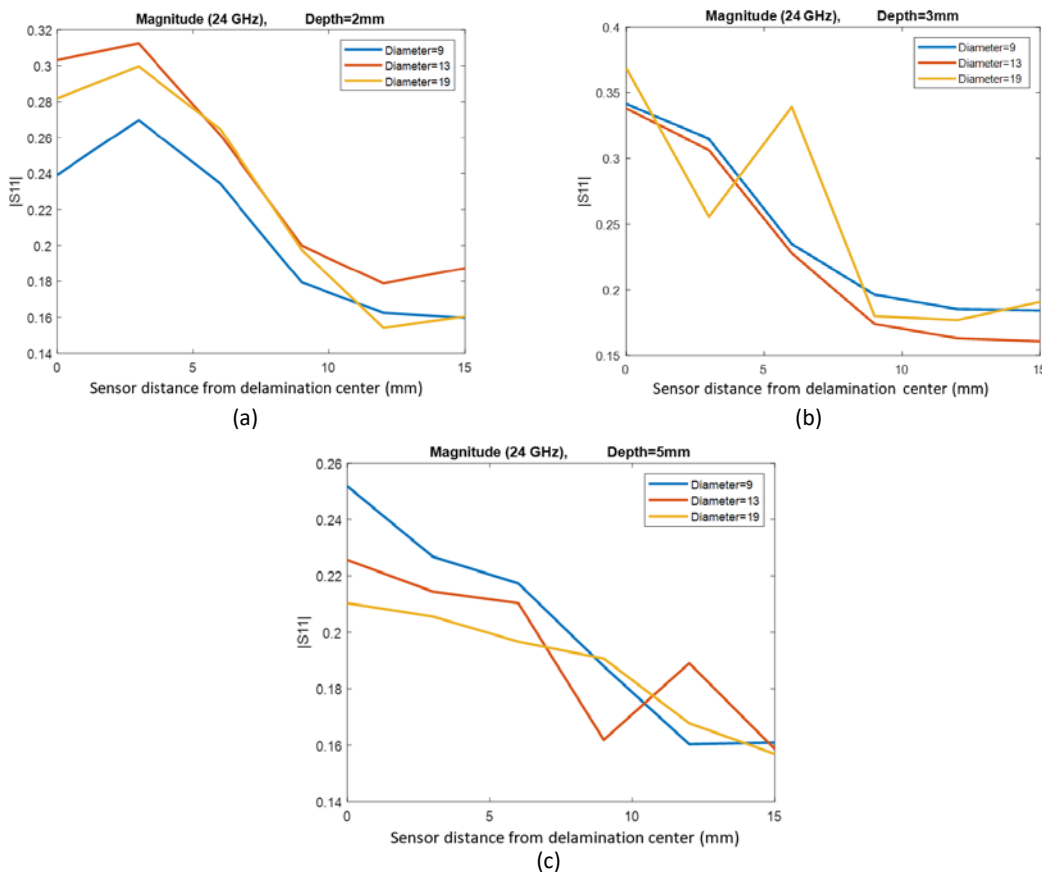


Figure 35: Simulated magnitude of reflection coefficient (S_{11}) at 24 GHz for three delaminations with diameters of 9, 13, and 19 mm, as a function of sensor distance from delamination center: (a) delamination depth of 2 mm, (b) delamination depth of 3 mm, and (c) delamination depth of 5 mm.

Task 2.8.2: Experimental Verification

A K-band (18-26.5 GHz) open-ended rectangular waveguide probe, connected to an Anritsu MS46131A [7] vector network analyzer (VNA), was used to scan sample 3 containing flat bottom holes (FBH) of various sizes from a lift-off distance of 10 mm, as shown in **Figure 36**. A vector network analyzer (VNA) is a laboratory grade benchtop piece of microwave equipment that is designed to produce the requisite irradiating microwave signal and receive the reflected signal. Once calibrated it gives the measured version of complex reflection coefficient, (S_{11}), for comparison with the numerical EM simulation results. **Figure 37** shows the measured reflection

coefficient (S_{11}), at various frequencies within the K-band (18-26.5 GHz) frequency range in both the magnitude-phase as well as the real-imaginary forms, as the open-ended waveguide probe scans three of the FBHs with different depths. As shown, the detection sensitivity of these FBH not only depends on their physical dimensions (depth and diameter), but also on the frequency used. For example, at some frequencies (e.g., 21 GHz) the sensitivity to the presence of FBH is very low. This corroborates the simulation results and further indicates the need for using some degree of operating signal bandwidth.

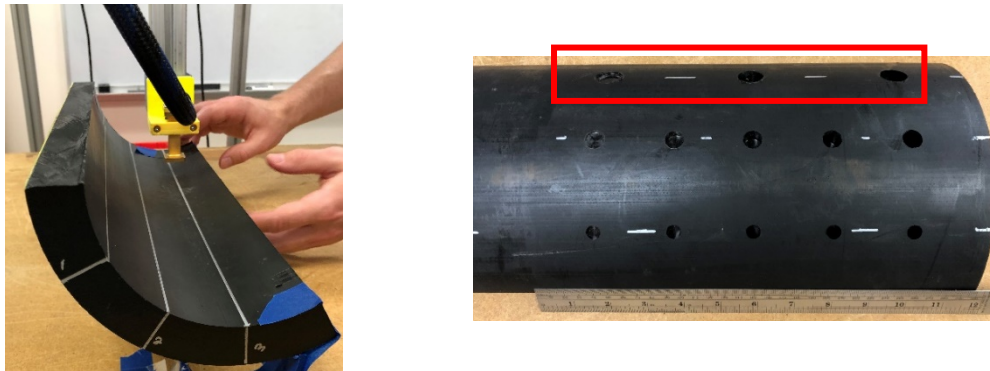


Figure 36: Picture of scan setup using a K-band (18-26.5 GHz) open-ended rectangular waveguide probe and an HDPE pipe section (sample 3) containing FBH.

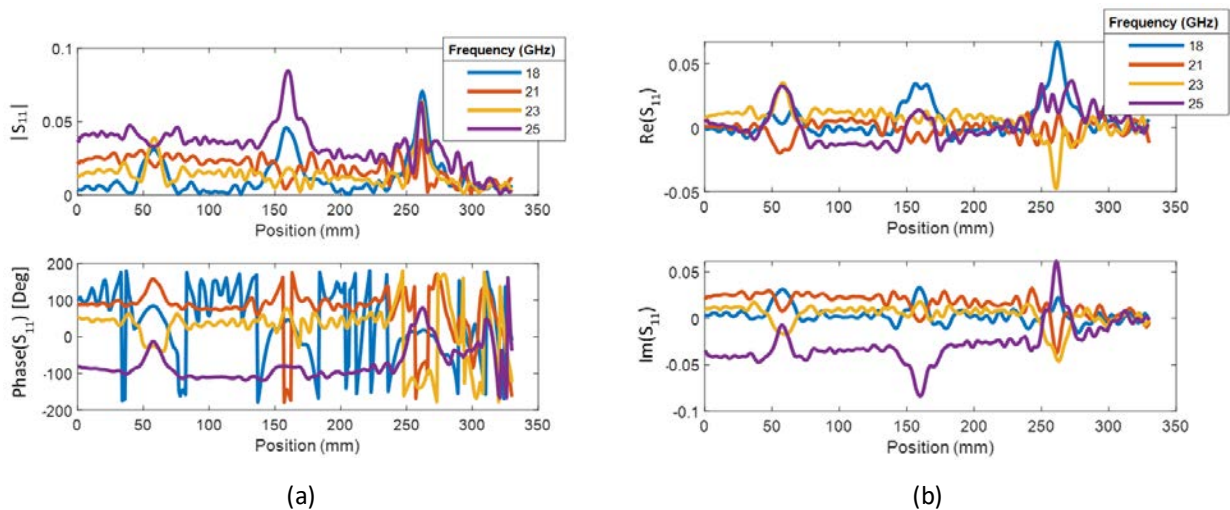


Figure 37: Measured reflection coefficient (S_{11}): (a) magnitude-phase and (b) real-imaginary forms, when scanning three FBHs using a K-band (18-26.5 GHz) open-ended rectangular waveguide probe.

These wideband measured data can be processed using a synthetic aperture radar (SAR) algorithm to create 3D images or slice images at different depths within the HDPE pipe [8]. However, it must be noted that the depth resolution associated with these images is limited to ~12.5 mm given the electromagnetic properties of the pipe material and the entire K-band (18-26.5 GHz) bandwidth used in the measurements. Generally, SAR imaging provides cross-range (i.e., lateral) image resolution of approximately quarter wavelength (~2.5 mm inside HDPE for K-band) when the depth of the target is smaller than the scan area. Detailed description of expected resolution can be found in the literature [8-9]. **Figure 38** shows SAR images represented as B-scan (cross-section representing signal across depth and scan path) where the Z-axis represent depth within the pipe wall and Y-axis represent scan path along the pipe wall in the axial direction for the three rows of FBHs in sample 3. As shown, the wideband SAR image shows indications of all FBHs and their depths within the pipe wall. The strong indication at Y=300 mm is due to reflections from the edge of this finite-sized pipe sample. **Figure 39** shows C-scan images representing raw magnitude at 24 GHz as well as SAR images focused at a respective depth of 24 mm and 30 mm within the pipe wall. The raw data shows indications of 4 out of 5 FBH (missing the deepest one), however the focused SAR images show indications of all 5 FBH. As explained in the simulation section, using a single frequency without SAR processing (i.e., raw data) can miss certain targets. However, this experiment clearly illustrates the benefit of using SAR imaging since this type of imaging takes advantage of coherent averaging of reflected signals received from all scan locations (i.e., spatial averaging) and also averaging over the entire frequency bandwidth of 8.5 GHz.

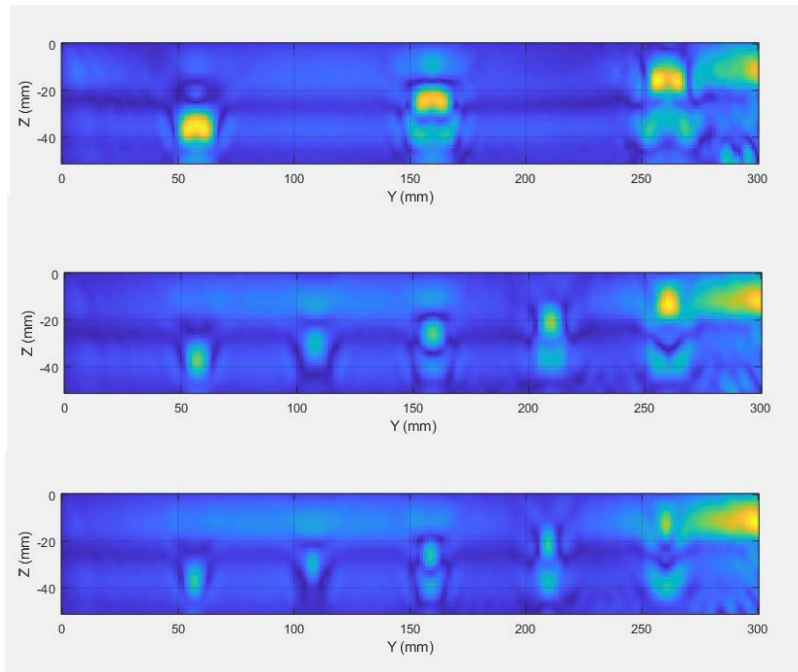


Figure 38: B-scan SAR images of the FBHs in sample 3. Z-axis represent depth within the pipe wall and Y-axis represent axial scan path along the pipe wall.

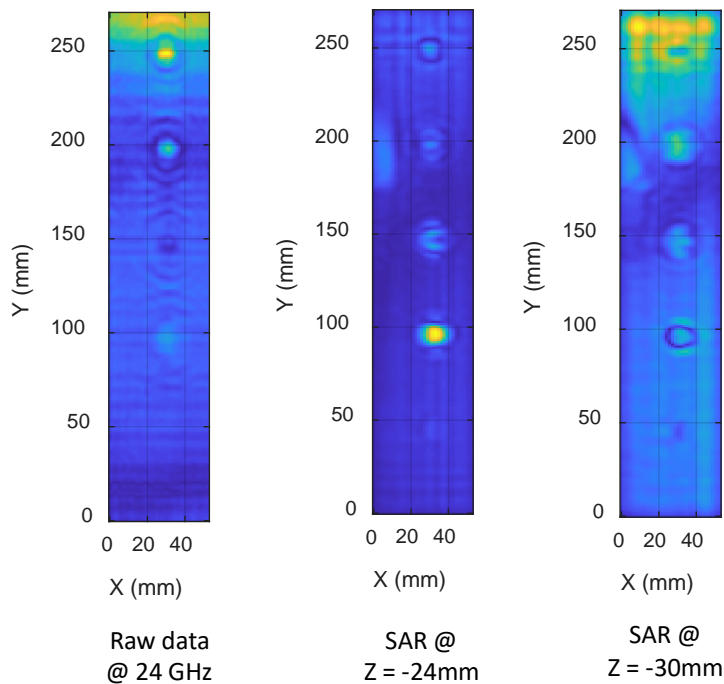


Figure 39: C-scan raw (data) images of the FBHs in sample 3. X-axis represent scan path along the circumference of the pipe and Y-axis represent axial scan path along the pipe wall.

In a real application environment, there are most assuredly objects such as rocks, roots and debris that come to contact with the outside wall of the pipe. These foreign objects may (most likely) reflect a larger signal back to the probe that is inspecting the pipe from the inside. Consequently, any reflected signal from a delamination, void, outside wall surface blisters, etc. within the pipe and near the exterior wall can be readily masked by the reflection from the foreign object. To illustrate this fact another imaging measurement was conducted in which a piece of Styrofoam, a piece of metal, and a rock were attached to the back of sample 3 and in between two FBHs, as shown in **Figure 40**. The sample was then placed on a bed of sand representing the backfill surrounding the pipe. The Styrofoam when placed in sand represents an air void since the low-density Styrofoam has properties similar to air at microwave frequencies. **Figure 41** shows the magnitude of raw data at 24 GHz for these three cases. As shown, large objects outside the pipe can produce strong signals obscuring indications of the adjacent FBHs, as shown for areas with Y in the 0 - 100 mm range (indicated by dashed red circles). Y represent the axial direction and X represent the circumferential direction. Furthermore, since single-frequency raw data does not allow for readily localizing targets in the depth direction, it is impossible to ascertain if the source of the signal is internal or external to the pipe. **Figure 42** shows the counterpart SAR images obtained using the wideband (18 – 26.5 GHz) reflection coefficient data. As shown, the SAR algorithm allows for focusing the images to an area internal to the pipe (e.g., Z=20 mm) where the objects outside the pipe are defocused. However, due to the limited range resolution of ~12.5 mm in the pipe, isolating the effect of strong scatterers such as the metal object remains difficult.

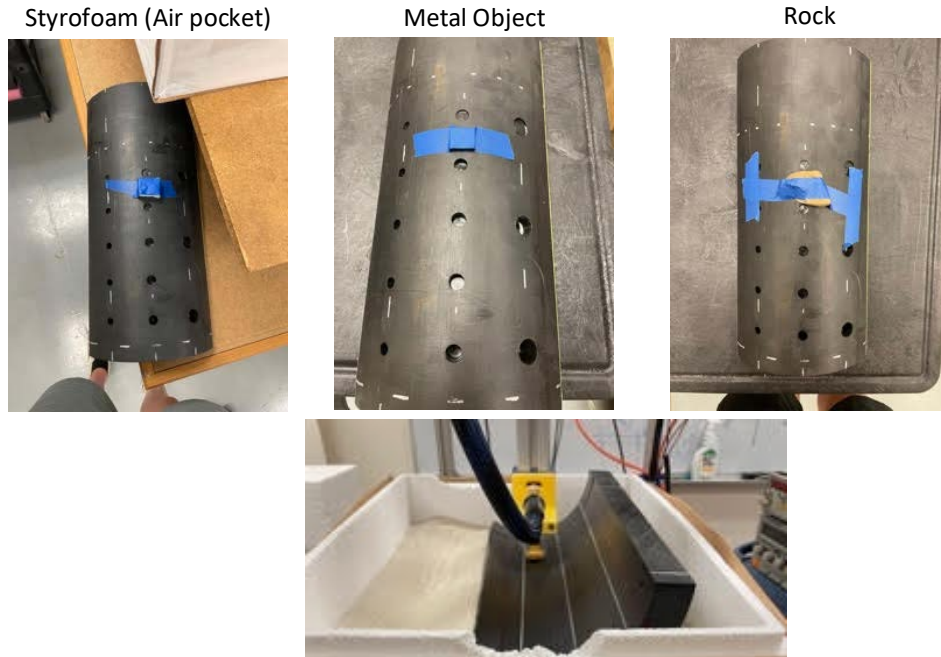


Figure 40: Picture of scan setup using a K-band (18-26.5 GHz) open-ended rectangular waveguide probe and a sample containing FBH on a bed of sand. Three separate foreign objects were placed behind the pipe (i.e., on outside wall) representing various external discontinuities.

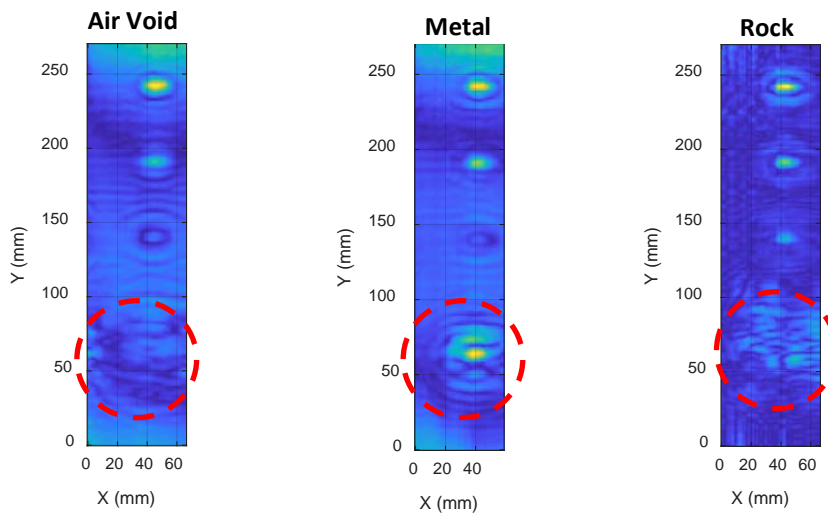


Figure 41: C-scan raw images at 24 GHz of FBHs in sample 3 when three different foreign objects are placed behind the pipe (i.e., on outside wall).

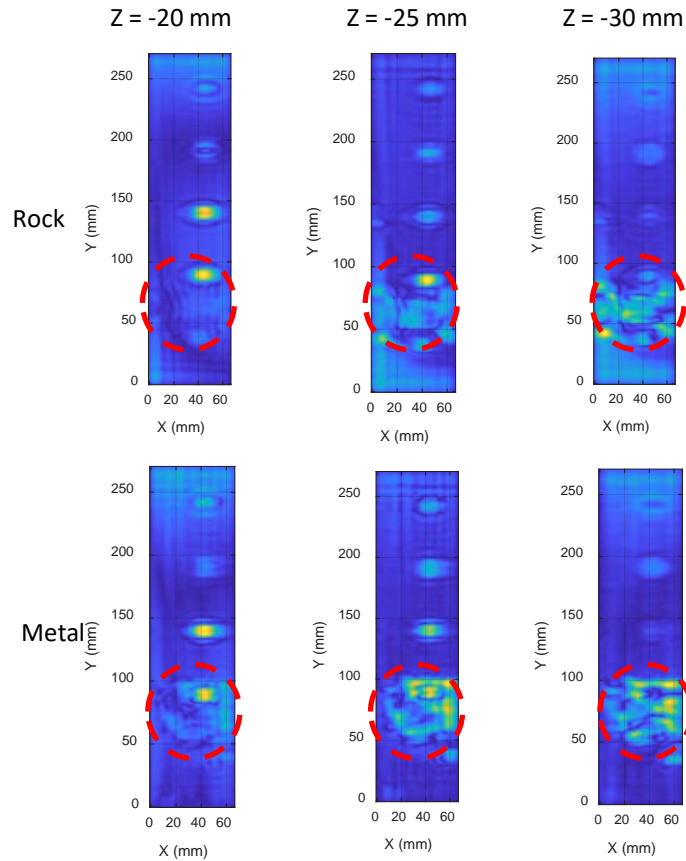


Figure 42: C-scan SAR images using wideband data of FBHs in sample 3 three different foreign objects are placed behind the pipe (i.e., on outside wall).

Task 2.8.3: Imaging Algorithm Optimization

We didn't employ any circular (or cylindrical) SAR imaging algorithm since we only dealt with sections of a pipe which could be approximated as a flat plane. When imaging a full circular pipe using a circumferential array, a circular (or cylindrical) SAR imaging algorithm in the polar coordinate can be employed. Such algorithms are available in the literature [10-13].

Task 2.8.4: Build Bench-Top Prototype Building Block

Based on outcomes of the simulations and measurements presented above, a radar sensor, based on the Infineon BGT24LTR11 radar IC, was designed operating at a frequency of 24 GHz

with a bandwidth of 2 GHz. The radar sensor is then encased in an aluminum package. The aluminum package serves as the open-ended rectangular waveguide probe (antenna) body and as an EM shield for the microwave electronics. The overall size of this sensor is 12.6 mm x 12.6 mm x 41 mm including the casing .

The sensor was built and assembled as shown in **Figure 43**. The frequency range of the sensor was tested using a spectrum analyzer and it was shown that it can reliably provide a frequency bandwidth of 22.7 – 24.7 GHz. Two sensors module prototypes were built. The first one showed intermittent instability that is believed to be due to damage to the Infineon IC caused by excess heating during the board assembly. The second, more stable, prototype was used for scanning several of the pipe samples. **Figure 44** shows a picture of the experimental setup showing the prototype sensor module being used to scan a section of sample 3 and the resulting SAR image. The resulting SAR image clearly shows the presence of the FBHs in this sample with very little (to no) background clutter in the image. **Figure 45** shows a picture of a section of sample 1 (containing small FBHs) and the resulting SAR image obtained using the prototype sensor module. The clutter at the bottom of the image is due to the reflections from the edge of the sample, which also aliases to the top of the image due to the Fast Fourier Transform (FFT) functions used in the SAR algorithm. **Figure 46** shows picture of a section of sample 2 and the resulting SAR image obtained using the prototype sensor module.



Figure 43: Pictures of the prototype sensor module with caliper showing dimensions in mm.

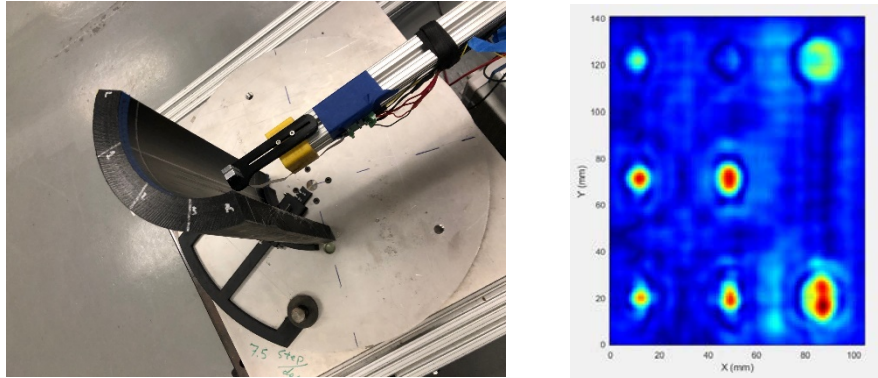


Figure 44: Picture of the experimental setup showing the prototype sensor module being used to scan a section of sample3 and the resulting SAR image.

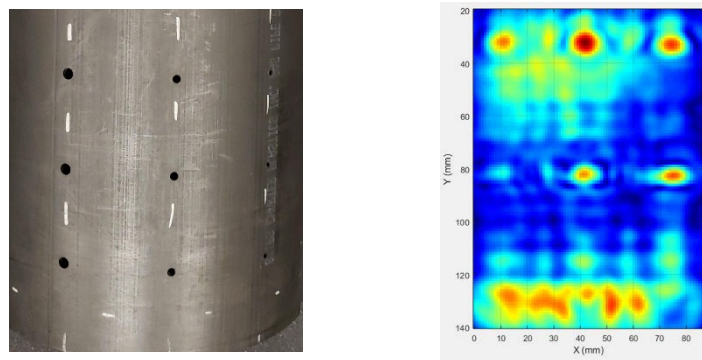


Figure 45: Picture of a section of sample1 and the resulting SAR image obtained using the prototype sensor module.

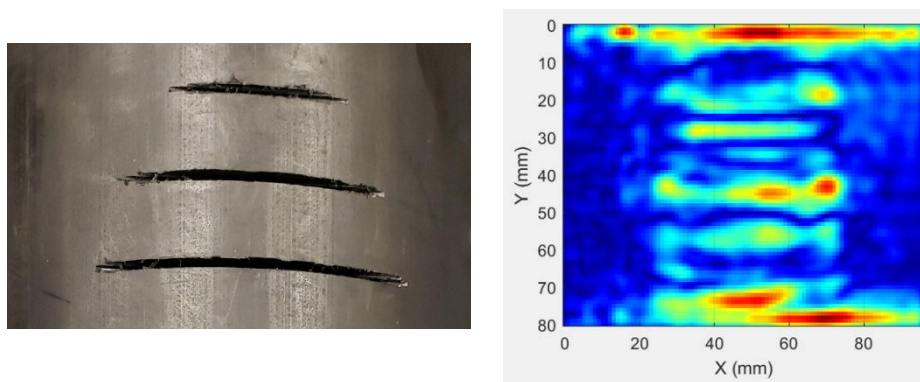


Figure 46: Picture of a section of sample 2 and the resulting SAR image obtained using the prototype sensor module.

Task 2.8.5: Design Specifications Study

It is envisioned that the microwave sensor will require two robot modules. One robot module would carry the sensor array and the other would carry the supporting electronics (data acquisition, control, and processing). For proper operation, we estimate that the robot needs to maintain the sensor modules centered within the pipe to within less than a millimeter.

TASK 2.9: FEASIBILITY AND DESIGN STUDY - ULTRASONIC INSPECTION METHODS

A modern UT inspection system consists of functional units that include a pulser/receiver, transducer and display device (see <https://www.nde-ed.org/NDETechniques/Ultrasonics/index.xhtml> for example). In systems intended to make multidimensional scans, additional components to move the transducer about the scan region and record data at each scan position are also included. In operation, the pulser dumps energy from a capacitor to the transducer, where an electrical-to-mechanical transduction occurs, generating high frequency sound (vibrational) energy that propagates into or over a part under inspection. During propagation, the sound energy is modified by the parts material condition. When the propagating sound energy impinges upon a significant acoustic impedance discontinuity (for example, sound impinging on a crack in a monolithic metal casting), some portion of the sound energy is reflected back toward the transducer, where a mechanical-to-electrical transduction occurs, which is captured by the receiver and either stored or displayed.

In the above description, acoustic impedance is the product of a material's elastic stiffness and density. In this manner, because the transduction processes are linear and reciprocal, the strength of reflected energy is proportional to the magnitude of the acoustic impedance discontinuity. Furthermore, the time for the sound to propagate to the discontinuity and back is related to the propagation distance by the material's ultrasonic velocity. In this manner, one can infer, for example, the depth of a discontinuity below an inspection surface. By propagating sound in different directions, the discontinuity size, orientation and other features can often be determined.

Task 2.9.1: Ultrasonic Materials Property Measurements

Measurements of the primary longitudinal and shear bulk mode velocities of propagations are typically the initial measurements made, as these are inputs to selection of operating settings used in subsequent testing (velocities determine refraction angles and gate placement in scanning). Longitudinal and shear velocities are the speeds at which these two modes (determined by particle displacement vector compared to propagation direction) travels through a given material. Additionally, these measurements give insight into the mode attenuation at various frequencies, which informs what frequencies are most appropriate for use. With measurements at various locations (and polarizations with respect to shear waves) on a pipe specimen, a range of expected variation and local anisotropy can be developed.

Velocity measurements were made by capturing multiple back-wall reflection echoes and determining the time delay between sequential echoes for both longitudinal and shear modes. Average values for longitudinal velocity were found to be 2370 m/s (± 16 m/s) and 906 m/s (± 12 m/s) for shear. It was found that shear velocity was not polarization dependent, indicating anisotropy in mechanical properties was minimal. **Figure 47** is typical A-scan showing the first and second longitudinal back wall echoes from a 5MHz contact probe. The time delay between the echoes (approx. 21 sec) and the sample thickness (1.00 in.) determine velocity (distance over

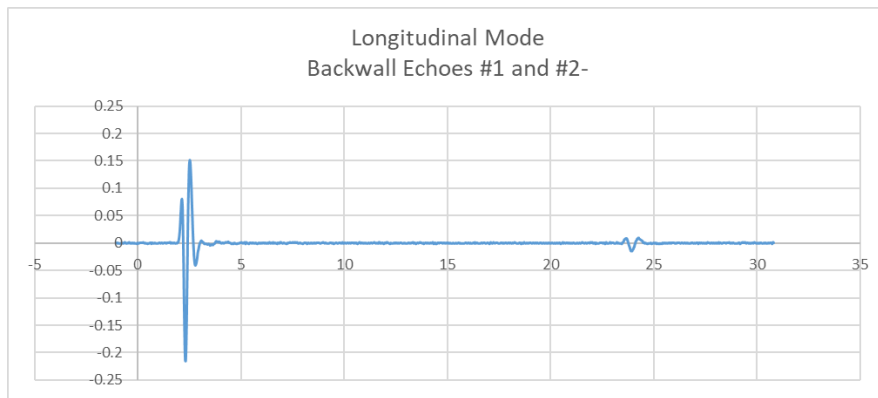


Figure 47: Typical A-scan showing first and 2nd backwall echoes using longitudinal wave probes at 5MHz. The time delay between echoes and the pipe sample thickness determine longitudinal wave velocity.

time). **Figure 48** shows A-scans from the first shear back wall echo (29dB gain used) and the 2nd shear back wall echo (49dB gain used, the 20dB gain difference represents a 10x difference in signal amplitude), with a delay between echoes of approximately 56 sec. The 20dB (10x) gain difference demonstrates that significant energy in the shear mode is lost during propagation. Attenuation of the longitudinal mode was relatively low, allowing 5MHz probes to be utilized on the thicker specimens (fortunately, as only 5MHz roller probes are available in the CNDE probe inventory). However, shear mode attenuation was roughly an order of magnitude higher than that seen for longitudinal mode at 5MHz, indicating that if shear modes are to be utilized, lower frequencies will be more appropriate.

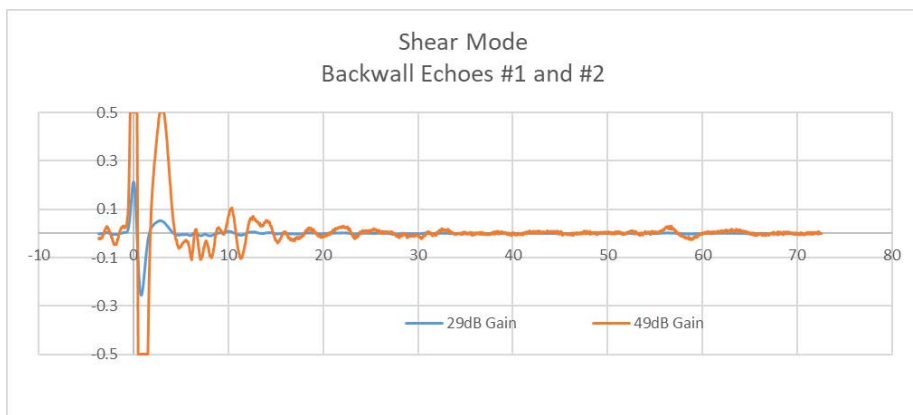


Figure 48: A-scan of shear wave first (blue trace) and 2nd (orange trace) back wall echoes using a 5MHz shear wave probe. Note that an increase of 20dB was needed to capture the 2nd back wall echo, demonstrating significant shear mode attenuation.

Task 2.9.2: Benchmark Measurements

To determine ultrasound-based detection and resolution limitations, the group of samples with engineered defects described earlier were used. The defects added were meant to simulate planar defects such as in-wall delaminations (circumferential-axial plane) and cracks (radial-circumferential plane). The pipe with naturally occurring outer skin delamination (from SouthWest Gas) was also used.

The in-wall delamination defects were fabricated by milling flat bottom holes of various diameters and depths from the inner pipe bore with end mills. Crack-like defects were made using

either rotary slotting cutters on a vertical mill or ground/shaped utility knife blades used like a stroke shaper on the vertical mill. The various defects were scanned (B-scan or C-scan) to demonstrate the detection/lateral resolution as well as depth discrimination capabilities.

Benchmark testing did not take place with the air-coupled components as it was determined early on that this coupling mode would be too inefficient and slow for the target pipe length scan rates. Immersion (liquid-coupled) approaches were also not benchmark tested here because any loss of liquid couplant into the operating gas stream was not tolerable (the so-called “dripless bubbler” type ultrasound configurations developed at CNDE do leak small amounts of liquid couplant, but even these small amounts are not acceptable). Roller probe testing was performed on a select group of the samples to demonstrate its capabilities. The roller probe was part of the Pocket UT system originally sold by Mistras, as shown in **Figure 49**. This system incorporates a portable single probe interface with pulser/receiver for ultrasound signals and displays processed results on the small screen on the instrument. The probe itself is comprised of a pair of 5MHz piezo crystals mounted in an axle and surrounded by an elastomer dry coupled wheel, which rotates on the axle. The configuration used is referred to a “pitch-catch” arrangement.



Figure 49: Pocket UT hand-held scanner with remote pulser/receiver/display unit and roller probe and cables.

Scans of the pipe samples were completed using both hand scanning of the Pocket UT system and scans with the roller probe removed from the hand scanner and mounted onto a lab scanner. The data collected was saved and output graphing. **Figure 50** shows selected hand scan results for two of the 8" pipe samples with flat bottom holes (FBH) drilled from the OD, with FBH hole diameters noted. The sample with the 1/2" FBH had depths of 0.1, 0.5 and 0.9 inches, where the sample with the 1/4" and 1/16" FBHs had depths of 0.1, 0.3, 0.5, 0.7, 0.9 inches. The intensity of the color in the B-scan image indicates signal strength, the horizontal width compares to the FBH diameter, and the vertical height indicates the depth of the FBH from the ID. The horizontal signal level along the top edge of the B-scan is the signal reflecting from the OD of the pipe.

The other samples fabricated, with narrow and wide notches, were also examined with the Pocket UT instrument. The physics of the propagating waves interacting with notches is identical to flat bottom holes, and in the display mode available in the Pocket UT these defect types also appear identical. Therefore, for brevity, they are not shown here.

With the roller probe removed from the Pocket UT cart and mounted to the end of a laboratory immersion scanner search tube, the 1/3 pipe sections of the 4" polyethylene pipe sample from SWG were mounted to a horizontal rotator, shown in **Figure 51**, and referred to as a X-scan.

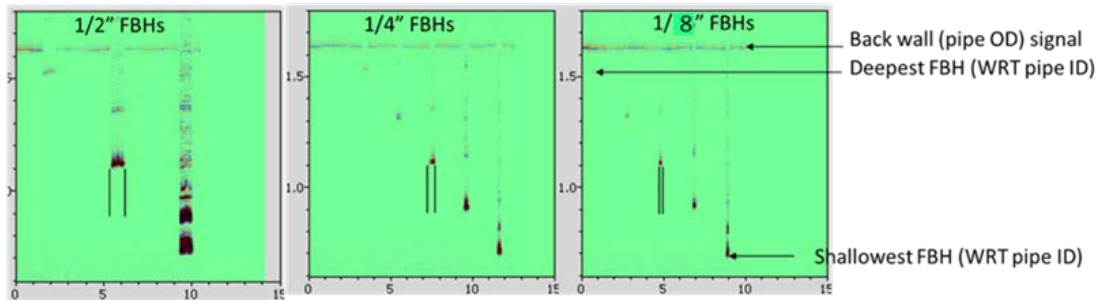


Figure 50: Hand scan results on FBH samples, showing B-scan results. Intensity of color is amplitude of received signals, position vertically indicates FBH depth.

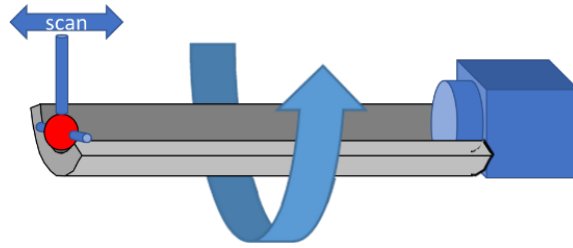


Figure 51: Diagrammatic view scanner setup for examining the SWG external blister samples, with roller probe moved along the length of the sample, with a rotator turning the sample. This is referred to as a X- scan.

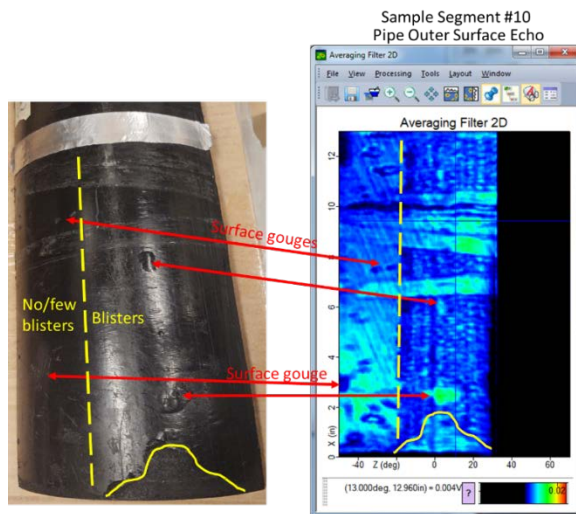


Figure 52: Photograph and roller probe C-scan results of SWG sample #10, showing response from outer skin blisters and regions with residual response from previous tape coverage.

Figure 52 shows results of this scan type on one of the SWG samples (sample #10) along with a photo of the sample. On the pipe were regions that had been covered by some type of tape or other covering, and this response was seen in the C-scan image result long after the tape was removed, along with both large and small blisters and surface gouges. The outer surface of the pipe sample could be notionally divided along its length, with one side having only a few blisters and the other side have a much larger blister condition. This is also seen in the ultrasound C-scan result. **Figure 53** shows similar results for sample #8.

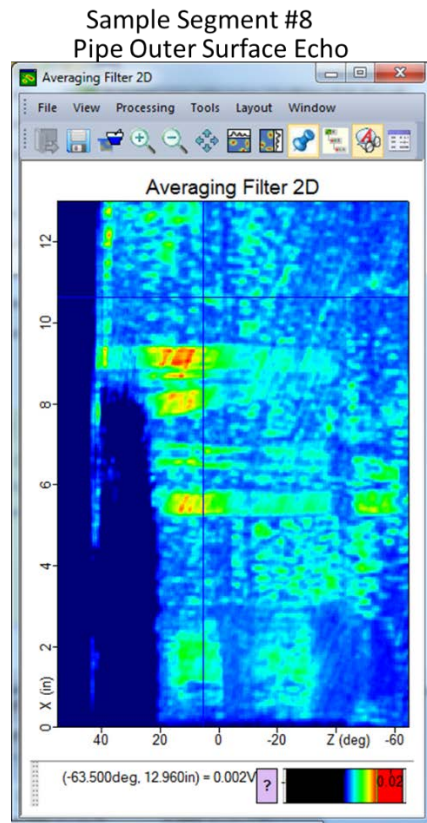


Figure 53: Rroller probe C-scan results of SWG sample #8, showing response from outer skin blisters and regions with residual response from previous tape coverage.

To compare the wheel probe response to what is expected to give the best single probe resolution, focused immersion inspection, scans of one of the SWG blister samples was scanned in an immersion tank (a large tank filled with water so to immerse the sample completely in the coupling fluid), using a 10MHz, 3/8” dia. focused probe, with the focal point on the outer pipe surface. The probe noted, with a higher frequency and focusing ability, was used to demonstrate the higher sensitivity achievable in through immersion approaches. A schematic of the setup is shown in **Figure 54**, with the resulting scan shown in **Figure 55**. The C-scan results shown is of much higher resolution and signal-to-noise, as expected. However, the roller probe results are

very good, considering that the probe arrangement is not optimized for polyethylene.

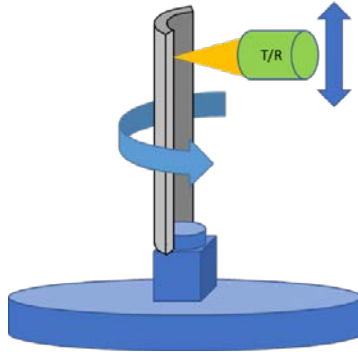


Figure 54: Diagrammatic view of immersion scanning setup, using focused 10MHz probe focused on OD of pipe at blisters.

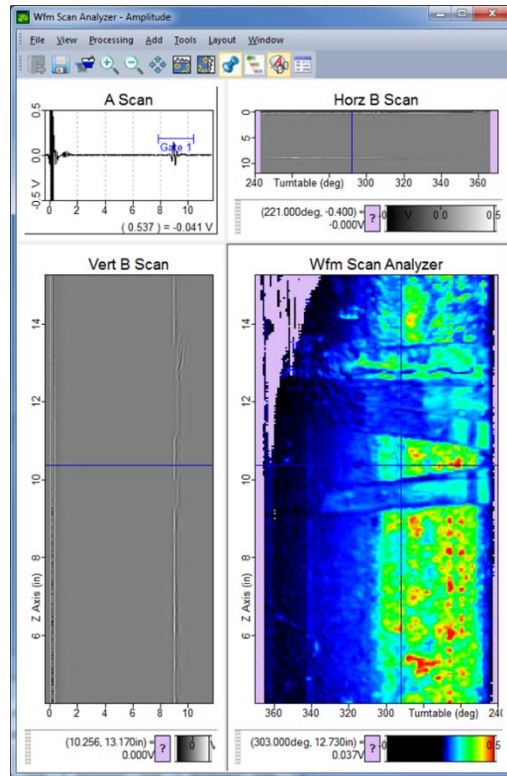


Figure 55: Immersion Scanning results on Sample 10 (as in Figure 9.2-5), showing similar by higher fidelity image as compared to roller probe.

Task 2.9.3: Survey of Available Commercial Components

For commercially available components to be considered in the design study, a survey of manufacturers was conducted. **Table 5** summarizes the components available as stock products (not custom designs) from the various manufacturers for the approaches considered in the design study. This summary represents a list of manufacturers to approach for fabrication of components on future phase II work if an ultrasound approach is selected

Table 5: Summary of suppliers of commercial components for considered ultrasound approaches.

Supplier	Air-Coupled components	Dry-Coupled Components	Captured Water column components
QMI, Inc.	Pulser/receivers and probes		
Ultran Group	Probes	Dry Coupled Probes	
Olympus Corporation		Elastomer sheets and delay lines (cylinders)	Miniature captured water column “bubblers”
Structural Diagnostics Inc.			Bubblers or Irrigated probe systems
Sonotec	Probes		
Starmans	Probes		
Eddyfi Technologies		R-scan dry-coupled wheel probe	
Innovation Polymers		Elastomer sheets, block and roller probe tires	
Mistras Group		Dry-coupled wheel Probes	

Task 2.9.4: Design Study

For the three possible approaches for deploying ultrasonic modes for pipe inspections (captured water column immersion, gas-coupled ultrasound, and dry-coupled roller probes), a

review of the typical applications, operating parameters and utility of each approach was evaluated. The captured water column coupling ultrasonic testing using standard immersion probes and air(gas)-coupled ultrasonic probes are both found in the literature for other applications and have been used extensively at CNDE for lab and field research.

The captured water column approach was developed at CNDE in the mid 1990's, under the project funded by the FAA aimed at improving inspection of fuselage skin lap joints for corrosion after the Aloha Airlines accident. The end product of this research, the so-called Dripless Bubbler, demonstrated the concept of a captured water column to hold a focused immersion probe, with only a thin dynamic layer of water to couple the end of the water column to the part under inspection. This dynamic layer of water was fed under pressure to the region between the water column and part surface, with a series of brush seals acting to form a chamber for the flowing water. Water leaking past the brush seals was vacuumed up and recycled.

When in use, most, but not all, of the water was successfully vacuumed and recycled. Typically, an hour's use would see on the order of 1 liter of water lost. Additionally, with continued use, atmospheric air would be entrained in the water, causing additional attenuation of the ultrasound in the coupling layer and also change the propagating wave speed, altering the focusing conditions. Inside a polyethylene gas pipe, with the pipeline in service, gas entrainment of the recirculating water would certainly be worse, and loss of the water coupling fluid into the gas stream would be problematic for the operator. Additionally, any sludge or contaminants within the pipe would also be swept up in the coupling water and could plug the jets injecting water into the chamber between the end of the water column and the pipe wall. Also, because the pipe needs full inner bore inspections, when in the upside-down position (inspecting top side of an installed pipe), any bubbles in the dynamic water layer, naturally buoyant, would tend to collect and not be swept away with the flow, blocking/scattering the sound beam. Higher water pressure and flow rates could help in this situation but would increase water lost outside the bubbler and into the gas stream.

CNDE began research using commercially available air-coupled ultrasonic probes in the early 2000's, at the request of NASA, to allow inspections of composite carriers for space missions. In the previous NASA approach, composite carriers were inspected in immersion, but required a bake-out procedure to ensure any water ingresses into the materials were removed prior to mission deployment, where it could freeze in the space environment and damage the material. Since this

work, CNDE has applied air-coupled ultrasonic testing to all manner of composites and polymer structures/materials.

At standard atmospheric pressure, the efficiency of air coupled probes is very low, with only about 1% of the total energy output of the probe entering the material under inspection. With this condition, the 99% of energy not entering the material is dissipated into the surrounding environment. Inside a pipe under pressure, the efficiency of the probes would increase but still be low. Probes could be redesigned for a particular pressure-level condition, but changes in pressure in the pipeline would cause the probes to operate off peak (designed) efficiency. Within the enclosed environment of the pipe, with each pulse of the probes, the ultrasound energy not entering the pipe wall would reflect around within the pipe cavity and would take several reverberations (hundreds of milliseconds) before the sound is sufficiently attenuated to begin another pulse of the probes, resulting in very slow scan rates (on the order of 100x slower than immersion or dry-coupled approaches). In the pipe, sludge or contaminants would tend to decrease the already low coupling between the gas and pipe. Finally, because the efficiency of the approach is so low, even under optimal conditions, probes are typically designed as transmitter/receiver pairs. In this way, a transmitter is optimized for production of sound, and a receiver is optimized as a sound sensor, typically with an amplifier built into the receiver probe. This approach necessitates always using a pair of probes for a single sensing channel (referred to as a pitch-catch setup), requiring double the number of probes as a single probe or pulse-echo setup. Finally, air(gas) coupled probes are typically lower in frequency to mitigate the attenuation effects attendant with propagating in the relatively low-density medium, which necessitates larger probe areas to generate planar propagating waves. The large probe surface areas will significantly increase the number of robotic scanner platform modules needed for full coverage of the pipe bore.

Dry-coupled probes have seen increased utilization due to R&D efforts in new elastomers that present low attenuation to ultrasound with low stiffness to conform to the coupling surfaces (probe face and part). While dry-coupling elastomer sheets work well to couple the probe and part, these are not easily translated/slid to facilitate scanning. However, the dry-coupled wheel probes provide a rolling translation of the coupling surfaces that works very well. Existing components originally offered by Physical Acoustics/Mistras [14] as the Pocket UT system are offered now by Eddyfi [15] as the Silverwing R-scan. CNDE has one of the original Pocket UT systems in inventory and used this system as originally configured. It was partially disassembled and

attached to a lab scanner for C-scanning of the defect samples fabricated at CNDE and the SWG sample. Scans of the 8-inch pipe sample with 1/4, 3/16 and 1/8-inch FBH's was tested. **Figure 56** shows results of this approach, where all of the FBH's were imaged in the scan. With an optimized design, much higher resolution (in lateral dimensions) and depth would be expected.

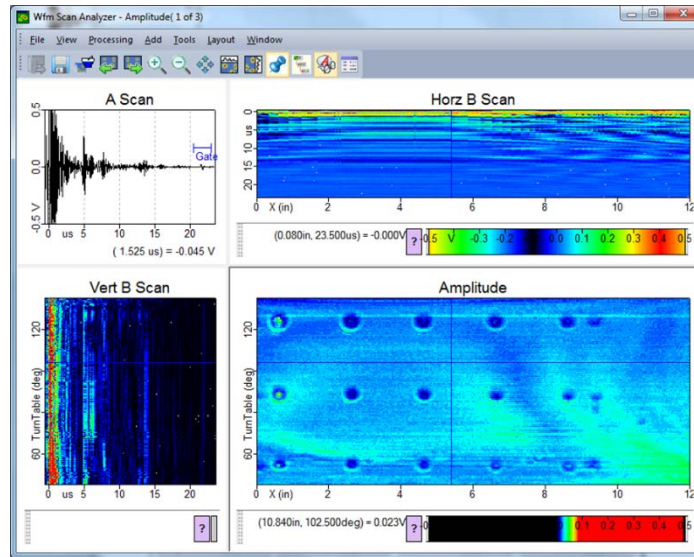


Figure 56: Pocket UT wheel probe scan using a single piezo element in a pulse-echo configuration, imaging FBH's of 1/4, 3/16, and 1/8-inch diameters at various depths., demonstrating that the roller probes should be able to incorporate additional piezo elements to increase scan coverage per roller probe.

TASK 2.10: DATA POST-PROCESSING, INTEGRATION AND SHARING AMONG THE NDE SENSORS

As described in Sections 2.7 - 2.9 above, various post-processing methods had been applied to the data acquired by each of the three NDE techniques under evaluation in this project using in-house developed software or commercial software provided by the vendors or purchased separately. Advanced signal and image processing techniques for enhancing the A-scan waveforms and C-scan images were being routinely utilized and, in broad sense, shared among these three NDE techniques. Since it is not known until later time which NDE technique(s) will advance to Phase 2, it is too early and unnecessary to consider data integration and/or data fusion in present phase. We defer such effort to Phase 2 when indeed two or more NDE techniques are selected to move forward.

TASK 2.11: FINAL NDE SENSOR(S) SYSTEM SPECIFICATIONS

After the detailed studies performed in Tasks 2.7 – 2.9 as described in Subsections 2.7 - 2.9 above, we arrived in an updated final set of specifications for the NDE sensory systems that will serve as the starting point of the follow up work once a particular system is selected.

TASK 2.12: CONCLUSIONS AND RECOMMENDATIONS

Overall Remarks

The ultimate goal of this effort has been to investigate the efficacy of three nondestructive techniques for inspecting low- and high-density PE pipes. This feasibility study is the first step in the development of potentially suitable and miniaturized NDE sensors which ultimately may be integrated with appropriate mobile robotic carriers, in a potential follow up endeavor.

The report has outlined the critical design aspects and performance of the three NDE methods (selected for concept development earlier in the project) and their ultimate potential efficacy for this application. Overall, the approaches and the outcomes of this investigation indicated that each of the three NDE methods has its own unique advantageous features as well as limitations. Moreover, sensor design miniaturization introduces certain unique design and application constraints that are not of concern in most other applications. As part of the sensor miniaturization efforts some design adaptations were considered and implemented.

Conclusions for each NDE method

Below individual conclusions and recommendations are provided for each of the investigated NDE techniques in this feasibility study effort.

Terahertz Imaging

THz, thanks to its exceptional temporal and spatial resolutions, demonstrated great ability in successfully detecting the defects embedded in the selected samples made for this project with high certainty. These samples cover both synthetic slot cuts, flat-bottom holes, surface air gaps, and naturally occurring delamination found in SWG field pipes. It should be pointed out that, in separate NYSEARCH-funded projects, THz has already detected very small naturally occurring indications in pipe wall and resolved delamination in real Driscopipe extracted from the field.

As depicted in our conceptual design, a THz pulsed inspection system, based on components available in the market, is estimated to be feasible to fit inside of 4” diameter pipe. Such THz inspection system is also estimated to be able to meet the minimum scan speed with sufficient resolutions in both axial and radial directions.

Microwave Imaging

Simulations and measurements showed the capabilities of microwave imaging for detecting flaws such as delaminations and crack-like notches in thick HDPE pipes. The experiments also showed that it is difficult to distinguish among external objects that are attached to the outside wall of the pipe such as: rocks and voids from defects on the pipe outer surface, which limits the sensitivity of microwave imaging for detecting defects near or on the external surface of the pipe. Overall, and based on the experimental results and the availability of commercial off-the-shelve (COTS) components, mainly radar systems on chip integrated circuits (ICs) and the possibility of designing small sensor arrays, the ISM frequency band around 24 GHz was chosen for the prototype sensor module. A prototype sensor module was designed, built and successfully tested. These tests indicated the feasibility of designing a sensor array that can fit in pipes with diameter as small as 4”.

Ultrasonic Inspection

Consideration of three ultrasonic approaches, including captured water column immersion, air (gas)-coupled ultrasound, and dry-coupled roller probes ultimately demonstrated that only the dry-coupled roller probe is a reasonable approach for use inside a pressurized gas pipe. The inefficiency and very slow scan rates eliminate air(gas) coupled approaches, and captured water column immersion, although offering the highest sensitivity/spatial resolution, any loss of the coupling fluid into the gas stream is unacceptable. The dry-coupled roller probes used still demonstrated good sensitivity and resolution, and when optimized, should offer excellent performance. In use, condensate in the pipe will not hamper the operation of the unit, although grit and similar dry/sharp granules would be expected to accelerate wear and gouging of the elastomer wheel, which would affect sensitivity and performance. The dry-coupled roller probe approach is the recommended ultrasound-based method for any follow-on studies.

8. IMPACT FROM THE RESEARCH RESULTS

This feasibility study has explored the possibility of developing a robotic inspection tool for the live, inline, non-tethered, non-destructive evaluation of polyethylene (PE) plastic pipes used in the natural gas distribution network. Various concepts were developed both for the robotic platform that will carry the sensors in the pipe and for NDE sensory systems that will carry out the actual inspection for defects.

The feasibility study has concluded that a 4” robotic system with NDE capabilities is the smallest robot we can build based of existing technologies that will meet most of the specifications set. A concept for a robotic platform was developed. Various communication options were explored and tested, and a concept was selected for further development in future phases. Regarding the NDE sensor, three different technologies were explored. It appears that microwave sensing is not suited to this application given the present state of the art. However, dry-coupled ultrasound and terahertz technologies show significant promise, each exhibiting advantages and disadvantages over the other. Further work is needed to determine which technology is optimal for this application. It was also determined that the commercialization of such a system will most likely take more than three years from completion of this work.

Given the need for technologies that will inspect plastic pipe in the nearest possible future, a feasibility study was undertaken to develop a 2” system that would not provide NDE capabilities but visual inspection only, and would not have the disadvantages of existing visual inspection systems that tend to damage the internal surface of the pipe. A concept for such an advanced system has been successfully developed through this work and its development has already been carried forward with funding from NYSEARCH. We expect to have this system in the market in early 2024.

In summary, this project has successfully developed concepts for advanced inspection systems for 2” and 4” PE pipes that would enhance the safety and operational efficiencies of the natural gas distribution network. Additional phases are needed to design, test, and commercialize the technology for the benefit of the natural gas industry and the public.

9. RECOMMENDATION FOR FURTHER WORK

The results from this project have provided us with a series of viable concepts for the development of two systems; one for the visual inspection of 2" PE pipes, and a second for the NDE evaluation of 4" PE pipes. Given the viability of these concepts it is recommended that we proceed with future phases for the development of each one of these two systems.

NYSEARCH has already funded a follow-up phase for the design, construction, and laboratory testing of the 2"-visual-inspection-only system. This work is now ongoing.

Another parallel effort is recommended to further develop the 4"-with-sensors-system. The knowledge being gained in the 2-inch-camera-only project will have an impact on the 4"-with-sensors concept design. Below is a set of tasks to be undertaken in a future Phase 2 of the 4"-with-sensors system that will provide for the design and laboratory testing of the system.

- Miniaturization of the current concept.
- Development of a launcher and retriever system for both 4-inch with sensor system and 2-inch camera only system.
- More investigation into possible module sizes based on launcher dimensions.
- NDE sensor integration.
- Optimize camera quality and image sensor (custom designed camera system).
- Integrate the 4-inch mechanical and electrical subsystems with the sensor modules.
- Develop a test loop/facility for ongoing test of design and deployment procedures.

A future Phase 3 will be needed after the completion of Phase 2 to carry out field tests and commercialize the technology.

10. FINAL FINANCIAL SECTION.

The project has been completed within budget and modified timetable. A no-cost extension was requested by NGA and was granted by PHMSA/DoT earlier in the project. The table below summarizes the project finances

Organization	Budget (as per proposal)	Final Expenditures
PHMSA/DoT	\$801,000	\$801,000
NYSEARCH/NGA	\$199,500	\$199,500

11. ACKNOWLEDGMENTS

NYSEARCH/NGA would like to acknowledge and thank PHMSA/DOT for its continued support of R&D efforts to develop this new inspection systems that would greatly enhance the safety and operational efficiencies of the natural gas distribution network. NYSEARCH/NGA would also like to acknowledge and thank Southwest Gas Corporation for its contribution to the project via its expertise and testing samples provided.

12. REFERENCES

- [1] Anon., Pipeline Safety Regulations, U.S. Department of Transportation, Pipeline Hazardous Materials Safety Administration, June 2004.
- [2] Patton, Thadd C., and David K. Hsu. "Recent Developments with the Dripless Bubbler Ultrasonic Scanner." In *Review of Progress in Quantitative Nondestructive Evaluation*, pp. 2045-2051. Springer, Boston, MA, 1996.
- [3] Redo-Sanchez et al., "Review of Terahertz Technology Readiness Assessment and Applications," *J Infrared Milli TeraHz Waves* (2013) 34:500–518 DOI 10.1007/s10762-013-9998-y.
- [4] Brinker K., Dvorsky M., Al Qaseer M. T. and Zoughi R., "Review of advances in microwave and millimeter-wave NDT&E: principles and applications" *Phil. Trans. R. Soc.* 2020, 378, 20190585-20190585 <http://doi.org/10.1098/rsta.2019.0585>
- [5] Ghasr, M.T. and R. Zoughi, "3D Millimeter Wave Imaging of Vertical Cracks and its Application for the Inspection of HDPE Pipes," *Proceedings of the 40th Annual Review of Progress in Quantitative Nondestructive Evaluation Conference, American Institute of Physics*, Conference Proceedings 1581, vol. 33A, pp. 1531-1536, 2014.
- [6] Ghasr, M.T., Y. Gao and R. Zoughi, "Handheld Microwave Imaging System for the Inspection of Non-Metallic Structures," Presented at the 46th Annual Review of Progress in Quantitative Nondestructive Evaluation (QNDE 2019), Portland, OR, July 14-19, 2019. (<https://www.iastatedigitalpress.com/qnde/article/id/8625/>).
- [7] <https://www.anritsu.com/en-US/test-measurement/support/downloads/brochures-datasheets-and-catalogs/dwl19970>
- [8] Case, J.T., M.T. Ghasr, and R. Zoughi, "Optimum 2-D Non-uniform Spatial Sampling for Microwave SAR-Based NDE Imaging Systems," *IEEE Transactions on Instrumentation and Measurement*, vol. 61, no. 11, pp. 3072- 3083, November 2012.
- [9] Liu, C., M.T. Al Qaseer and R. Zoughi, "Influence of Antenna Pattern on Synthetic Aperture Radar Image Sidelobe Level in NDE Applications," *IEEE Transactions on Instrumentation and Measurement*, vol. 70, pp. 1-6, January 2021
- [10] B. Wu, Y. Gao, J. Laviada, M. T. Ghasr and R. Zoughi, "Time-Reversal SAR Imaging for Nondestructive Testing of Circular and Cylindrical Multilayered Dielectric Structures," in *IEEE Transactions on Instrumentation and Measurement*, vol. 69, no. 5, pp. 2057-2066, May 2020.
- [11] J. Laviada, B. Wu, M. T. Ghasr and R. Zoughi, "Nondestructive Evaluation of Microwave-Penetrable Pipes by Synthetic Aperture Imaging Enhanced by Full-Wave Field Propagation Model," in *IEEE Transactions on Instrumentation and Measurement*, vol. 68, no. 4, pp. 1112-1119, April 2019.
- [12] L.-W. Li, M.-S. Leong, T.-S. Yeo and P.-S. Kooi, "Electromagnetic dyadic Green's functions in spectral domain for multilayered cylinders", *J. Electromagn. Waves Appl.*, vol. 14, no. 7, pp. 961-985, 2000.

- [13] G. Jia, M. F. Buchroithner, W. Chang and Z. Liu, "Fourier-based 2-D imaging algorithm for circular synthetic aperture radar: Analysis and application", *IEEE J. Sel. Topics Appl. Earth Observ. Remote Sens.*, vol. 9, no. 1, pp. 475-489, Jan. 2016.
- [14] Physical Acoustics/Mistras Group, Inc., 195 Clarksville Road, Princeton Junction, NJ 08550 USA
- [15] Eddyfi Technologies, 3425 Rue Pierre-Ardouin, Québec, QC G1P 0B3, Canada.

13. APPENDIX 1

Task 2.5: Technology review – NDE Sensor Techniques

This report is the deliverable for *Task 2.5: Technology Review – NDE Sensor Techniques*, which is part of the work scope of the project “Feasibility Study for Sensor Systems for In-Line Inspection of Plastic Pipe: NDE Sensor Development by ISU-CNDE” funded by NGA/NYSEARCH and the USDOT/PHMSA. The task description in the proposal is as follows: “We will perform a limited literature search, pertinent to the objectives of this particular inspection and as it relates to NDE methods that are already in use or have demonstrated real promise for utility. This technology review shall be conducted within the first 3 months of the project. The outcome of this task will be a succinct report, in the form of a “trade-off table”, outlining each method’s advantages and limitations. This effort will only concentrate on inspection-related issues and not those related to how the methods may be incorporated into a robot, etc. “

The NDE technologies reviewed for potential applicability in the application considered here, *i.e.*, inline inspection of natural gas plastic pipe, were: radiography (X-ray), eddy current, magnetic particle, electromagnetic acoustic transducer, shearography, thermography, air-coupled ultrasound, captured volume ultrasound, dry coupled probe ultrasound, microwave, and terahertz. Following are the reviews and general conclusions as per their applicability on the problem under consideration for each technique.

Radiography

How it works

Radiography or X-ray utilizes the principle of radiation’s interaction with matter to penetrate materials. High energy radiation such as gamma rays and X-rays are capable of penetrating many materials and this phenomenon is used for NDE imaging purpose. These high energy rays are transmitted through the sample material and absorbed based on the interactions with the sample’s molecular structure. High density materials will have more interactions and will absorb more energy faster as compared to light, low density materials such as air or human tissue. For medical applications, X-rays of bones are done using this same phenomenon to image bones under skin, tissue, and other organic materials. Density also affects the depth of absorption. Higher density will result in less depth of radiation penetration since there are more particle interactions and vice versa. Based on the varying intensity of the transmitted radiation, the sample can be imaged to show a density map indicating any defects such as cracks or holes.

Application to plastic pipe inspection

X-ray inspection of plastics uses the same principle as medical radiography for penetrating solid plastic objects. The Welding Institute (TWI) has done research in this area of plastic pipe weld inspection and published a study on the use of X-ray for examining polyethylene pipe welds.

Standard x-ray inspection of metals requires X-ray energy of 300 kV. However, plastics are less absorbent of X-ray energy so they require less intense x-rays to transmit through the material. TWI's study analyzed pipes by transmitting x-rays from inside the pipe outwards onto radiographic film placed on the exterior. The study concluded 16 and 26 kV X-rays were optimal for polyethylene pipes 5-50 mm thick. TWI also stated the ability to discern imperfections in the weld such as dust, gaps, and cold weld, seen in the x-ray image. This method can yield high quality images for visually finding imperfections in a weld or defects such as cracks and holes. However, both the inside and outside of the pipe need to be accessible for transmitting x-rays through the material onto receiver, as are most X-ray systems nowadays. Multiple safety precautions and trained professional handling is also required for operation due to the dangers of radiation and high cost of X-ray machines.

For this application, the biggest obstacle remains to be the equipment size, as both X-ray source and receiver are required to be inside the pipe to perform inspection in reflection (back-scattered) mode. Given the current technological state of radiography, it is still not possible to reduce the size of X-ray equipment to fit inside an 8" diameter pipe for example, while maintaining sufficient performance; the ongoing efforts in miniaturizing back-scattered X-ray system have resulted in systems with degraded resolutions.

PROS	CONS
<ul style="list-style-type: none"> • Industry standard for spatial resolutions • Useful for almost any material, especially plastics • Discerns varying densities in materials caused by porosity, cracks, or voids in welds • Identifies both surface and subsurface defects • Compared to metals, plastics are less absorbent of radiation and require lower intensity rays 	<ul style="list-style-type: none"> • Costly and bulky • Requires professional handling and many safety precautions for dealing with radiation exposure • Limited accessibility: access to both sides (inside and outside) of pipe is needed

References:

1. https://www.ndt.net/article/twi/twi_2.htm
2. <https://www.nde-ed.org/NDETechniques/Ultrasonics/Introduction/description.xhtml>
3. [https://www.esabna.com/us/en/education/blog/radiographic-and-ultrasonic-testing-of-welds.cfm#:~:text=Radiographic%20Testing%20\(RT\)%20%E2%80%93%20This,as%20that%20for%20medical%20radiography.](https://www.esabna.com/us/en/education/blog/radiographic-and-ultrasonic-testing-of-welds.cfm#:~:text=Radiographic%20Testing%20(RT)%20%E2%80%93%20This,as%20that%20for%20medical%20radiography.)
4. <https://www.tedndt.com/products/x-ray/>

Eddy Current

How it works

Eddy current (EC) testing is a contact electromagnetic technique commonly used for inspecting electrically conductive materials. It works by applying alternating electric current to coil roll (as probe) to generate a changing magnetic field, which in turn generates EC in the conductive test sample. The presence of defect interrupts the flow of EC and hence its strength. By monitoring this strength change, EC can then be used as a viable tool for flaw detection.

Eddy current measurements are typically plotted on the “impedance plane” whose horizontal axis denotes the resistance and vertical axis represents the inductive reactance. When placing the probe down on the sample surface and sweeping through it, a unique signal trace on impedance plane can be seen which correlates to the presence of a defect or the thickness of the material. During testing an EC system requires frequent “balance” or “zero out” which is done by taking measurement from a defect-free sample of the same material. EC responses can also be calibrated via “lift-off”, i.e., moving the probe on and off the sample. EC can inspect for thickness, coating/paint thickness, as well as detect surface and near surface flaws.

Application to plastic pipe inspection

The use of eddy currents in plastics is limited because plastics are typically good insulators of electricity. This means that eddy current inspection of PE pipe is not feasible given its lack of electric conductance.

Magnetic Particle

How it works

Magnetic particle examination is mainly for ferromagnetic materials such as iron and steel. The technique utilizes the magnetic properties of the material and its ability to transfer the magnetic flux, or field, without interruption. If there is a defect in the sample, such as a crack, the flux will leak shown in the image below. At this leak point the magnetic field exits the material at the north pole and reenters into the south pole causing the field to spread out a create a “flux leakage field”. Using this phenomenon, small magnetized iron particles, are applied onto the surface and will cluster at the poles and flux leakage points, visually indicating a defect at that point.

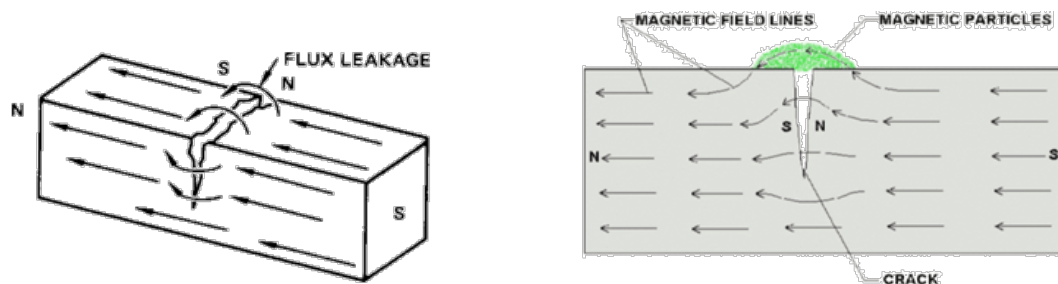


Image source:

1. <https://www.nde-ed.org/NDETechniques/MagParticle/Introduction/basicprinciples.xhtml>

Application to plastic pipe inspection

Due to the nature and principles of this method, it will only work with ferromagnetic materials. The samples need to be able to transfer a magnetic field. Polyethylene pipes consist of polymers that have no magnetic properties, so the magnetic particle method will not work for this material.

Electromagnetic Acoustic Transducer (EMAT)

How it works

Electromagnetic Acoustic Transducer (EMAT) generates acoustic waves inside of conducting materials. EMAT does not need direct coupling like UT and other methods, which makes them useful in difficult environments where contact or coupling can negatively affect the sample. EMAT uses a magnet and an electric coil, which generates a magnetic field and an AC electric field driven at ultrasonic frequency, respectively. The electric signal can be modified for specific applications from 20kHz to 10 MHz using continuous wave, spike pulse, or tone-burst signals. The driven electric field also creates a matching magnetic field, which in turn interacts with the constant magnetic field generated by the magnet. When these fields interact, they generate ultrasonic waves in the sample. This can only be done using the Lorentz force in conductive materials and magnetostriction when the material is ferromagnetic. EMAT is primarily used in metals manufacturing, automotive, railroad, pipeline, and pressure vessel industries. In addition to all the advantages of UT, EMAT does not require coupling, less sensitive to surface conditions, and easier to deploy the sensors. Its downsides are low transduction efficiency and the need for more signal processing. Furthermore, the transducers can be bulky, and caution must be taken with the magnets near steel and magnetic materials.

Application to plastic pipe inspection

EMAT would be a very good candidate for us to investigate welded joints of pipe samples if they were made of metals. Because our research is with HDPE pipes, EMAT will not be a viable method for inspection.

References:

1. <https://www.sciencedirect.com/science/article/pii/S0963869505000769>

Shearography

How it works

Shearography works by using lasers and cameras to detect stress concentrations on the surface of a sample. This is done by shining laser light on the surface of a part when there is no load applied to it. A camera then takes a picture of the surface and captures a speckle pattern that will be used

as the reference. Once the first image is taken, the load is applied to the sample and a second image is taken. The second image also has a speckle pattern which is then subtracted from the first to create an interference pattern. This pattern is then used to determine the presence of the defects and to identify the types of defects as well. Even and regular patterns show a flaw free area, while a location where the pattern is irregular and does not follow the standard pattern indicates a flaw. One advantage that shearography has over other techniques, in normal applications, is the scanning speed that it can operate at. It can scan in the ballpark of 1 square meter per minute while producing easily interpretable results in good detail, if sufficient lift-off distance is maintained and the part to be inspected is fairly flat.

Pros	Cons
<ul style="list-style-type: none"> • Non-contact • Rapid full-field inspection • Good Portability • Used on many different composites and rubbers • Excellent before ground installation • Laser is nonionizing • Simulating service stress can show service relevant flaws 	<ul style="list-style-type: none"> • Difficult to differentiate parts already stressed • Stress could cause damage • Surface cannot be optically smooth • Needs a large area to work efficiently • Requires sufficient lighting inside the pipes • Pipe’s tight curved geometry makes precise loading and uniform image measurements difficult

Application to plastic pipe inspection

There were numerous studies of the use of shearography to inspect composite patches on metallic pipes as well as studies looking at the use in various types of composites and rubbers. These studies found that shearography excelled at finding defects in the materials studied, which leads to the hope that the inspection of plastic pipes could be feasible. However, shearography has long been known as a qualitative rather than a quantitative technique, and there is not much information in the published literature about using shearography for plastic pipes inspection.

For the application of shearography to the inside of a plastic pipe, the cylindrical geometry of pipe with tight curvature results in shearography losing its advantage significantly as a full-field technique. This is particularly true when considering the spatial resolution and sensitivity required in this project. The minimal standoff distance between laser and surface being inspected effectively reduces to only the pipe ID, as compared to several meters in typical applications. The capturing of surface displacement responses in the loaded and unloaded conditions could likely only be accomplished by heat application, and with the low thermal conductivity of the plastic piping materials, the slow heating (and subsequent slow cooling before the next measurement) would severely limit scanning/inspection speeds. Indeed, according to the references provided, “significant feature of the configuration that was tested is that it is not applicable to small

diameters.”

References:

1. <https://www.twi-global.com/technical-knowledge/faqs/what-is-shearography>
2. https://www.ndt.net/article/wcndt2004/pdf/optical_techniques/753_hung.pdf
3. <https://www.sciencedirect.com/science/article/pii/S02954939501103X>
4. <https://www.sciencedirect.com/science/article/pii/S0143816617303603>

Thermography

How it works

Thermography uses a relatively large thermal energy flux to excite the surface of a sample and a thermal imaging camera to view the sample. Energy sources that are commonly used are halogen lamps, flash lamps, or ultrasonic horns. The thermal camera can track the heat dissipation into the sample and that can in turn be used to identify flaws and artifacts. This method is non-contact, which means it does not interfere with the sample or change its properties in any way. Some other advantages are that it can be used to view a larger area, it can measure moving objects, and it has a wide range of temperatures and configurations it can be adapted to, and results can be captured and analyzed very quickly. A perfect sample will absorb and distribute the heat evenly and in a way one would expect, but flaws, cracks, and inclusions can interfere with that heat flow. A large hole on the back surface, for example, will allow the heat to flow out of the sample and cause a hot spot in that area. A trapped bubble or internal crack will cause the heat to flow around it and therefore highlight the perimeter of the flaw with a hotter region.

Application to plastic pipe inspection

Thermography has been used on plastics and there are already a number of applications such as the inspection of injection molded parts, laser welding in the automotive industry, and PVC pipes. This technique allows us to see into the material and identify flaws, and if the heat dissipation rate is known, one can identify the depth and type of flaws with great accuracy. Thermography was also used to map the contact effectiveness of plastic welded joints to predict tensile strength and bond thickness with success.

For the current application in inspecting plastic pipes, however, thermography's inability of penetrating into pipe wall becomes a major problem. Given a typical inspection time window, the general rule of thumb for thermography's penetration depth of typical solid is only "a few millimeters" and worse for plastics for their lower thermal conductivity. The lower thermal conductivity in turn prolongs the heating and cooling time and severely reduces the scan speed. When confined inside the pipes with small space and tight curvature, thermography, similar to shearography, also significantly loses its advantage as a full-field technique. Taking all these shortcomings into account, thermography does not seem to elevate itself to the same level of the leading NDE techniques for this application.

Pros	Cons
Can view large areas	Sample thickness limits applicability
Can track moving objects	Equipment expensive and delicate
Large temperature range capabilities	Large energy sources are needed
Quick data acquisition and processing	The sample must absorb/transmit/reflect the input energy well
Many configurations for specific analysis	limited access complicated geometry

Air-Coupled Ultrasound

How it works

Air-coupled ultrasound is analogous to other ultrasonic NDE methods, where mechanical vibrations are coupled into the part or material of interest and evaluated by gauging how the vibrations (sound) are modified by the interaction with the part or material. The difference is the medium for coupling the mechanical vibrations, which is air or other gas. In this approach, the transmitting and receiving probes are purposely optimized for the low acoustic impedance of the coupling air or gas. Although this optimization greatly increases the efficiency of the probe output and sensitivity, the entire process is still very low in efficiency compared to, for example, contact or immersion ultrasound. To achieve the highest efficiency, low frequencies are used to minimize the attenuation effects attendant in air or gas. The lower frequency piezo elements, due to being thicker, also produce higher particle displacements (amplitudes), increasing available acoustic power. However, lower frequency probes require larger active diameters, making small aperture probes difficult to fabricate and optimize, and sacrificing spatial resolution. All manner of inspections, using focused or unfocused probes, various beam angles and modes are still available with air-coupled UT, just at lower frequencies.

Application to plastic pipe inspection

At standard atmospheric pressure, the efficiency of air coupled probes is very low, with only about 1% of the total energy output of the probe entering the material under inspection. With this condition, the 99% of energy not entering the material is dissipated into the surrounding environment. Of that 1% of energy that enters the material under inspection, only about 1% of that propagates outside the material and is received by the air coupled probes, making the process efficiency on the order of 1 part in 10,000. Inside a pipe under pressure, the density and acoustic velocity of the gas increases and hence decreases the transmission losses between the probes and the gas and the gas and pipe wall, increasing the overall efficiency of the transduction/propagation process but it is still quite low. Probes could be redesigned for a particular pressure environment, but changing pressures in the pipeline would cause the probes to operate off peak (designed) efficiency. Within the enclosed environment of the pipe, with each pulse of the probes, the 99% of ultrasound energy not entering the pipe wall would reflect around within the pipe and would take

several reverberations before the sound is sufficiently attenuated to begin another pulse of the probes, resulting in very slow scan rates. In the pipe, sludge or contaminants would tend to dampen or scatter the already low signal levels. Finally, because the efficiency of the approach is so low, even under optimal conditions, probes are typically designed as transmitter/receiver pairs. In this way, a transmitter is optimized for production of sound, and a receiver is optimized as a sound sensor, typically with an amplifier built into the receiver probe to minimize noise pickup. This approach necessitates always using a pair of probes for a single sensing channel, limiting the space available within the pipe bore for additional sensing channels. It is expected that the low very slow scan rates due to internal reverberation, changes in efficiency/sensitivity due to changing gas pressures and large probe footprints make this approach marginally applicable to in-service polyethylene pipe inspections.

Captured Water Column Ultrasound

How it works

With immersion ultrasound, a part needing inspecting is immersed in a coupling fluid, typically water. The coupling fluid acts as a low attenuation propagation path for sound to travel from the inspecting probe to the part, interact within the part, and then reflect or scatter backward to be captured by the probe. The acoustic impedance of water is typically lower than that of the materials being inspected, causing losses in transmission, but not so low as to inhibit inspections. With waters low attenuation and wave speed, higher frequencies and all manner of angled beams and mode conversions are possible, allowing for a large range of inspection modalities.

When parts become larger, it is of course not possible to immerse them, and so the concept of a captured water column that moves with the probe outside of an immersion tank was suggested. The water column approach was developed at CNDE in the mid 1990's, under the project funded by the FAA aimed at improving inspection of aircraft fuselage skin lap joints for corrosion after the Aloha Airlines accident. The end product of this research, the so-called Dripless Bubbler, demonstrated the concept of a captured water column to hold a focused immersion probe, with only a thin dynamic layer of water to couple the end of the water column to the part under inspection. This dynamic layer of water was fed under pressure to the region between the water column and part surface, with a series of brush seals acting to form a chamber for the flowing water. Water leaking past the brush seals was vacuumed up and recycled. When in use, most, but not all, of the water was successfully vacuumed and recycled. This approach allowed all manner of acoustic inspections with focused or unfocused probes, in normal incidence and angled beam configurations, utilizing longitudinal, shear, Lamb and Rayleigh modes.

Application in plastic pipe inspection

Inside a polyethylene gas pipe, with the pipeline in service, gas entrainment into the recirculating water in the dynamic layer would certainly occur and cause some degree of attenuation losses, most notably at the higher frequencies. If lower frequencies can be used in the detection of the defects of interest, this attenuation issue is moot. Any sludge inside the pipe that

is washed away in this recirculating water would need to be filtered out or risk plugging the jets into the dynamic water column chamber.

When operating upside-down (inspecting the top of the pipe) there is a possibility of introducing bubbles into the ultrasonic beam that would rise to the top of the dynamic layer, but higher water recirculation pressure and flow rates can minimize or eliminate this issue (the Dripless Bubbler was used successfully on the belly of aircraft to inspect for corrosion damage). The primary concern is loss of the dynamic coupling water outside the recirculation system into the gas stream. Most loss would occur at abrupt changes in pipe ID geometry, such as fittings and joints, and it is expected that elastomer seals could be used in-lieu of the original brush seals. It may also be possible to leverage the ambient gas pressure to minimize loss past the seals, but it is expected that any loss of water cannot be tolerated in this application.

Dry-coupled Probe Ultrasound

How it works

In all ultrasound applications (save EMATS), a coupling medium is needed to transmit vibrations (sound) from probe to part and back again for signal detection. Gels are used with contact probes (common in medical ultrasound), water and gasses have been discussed previously, and each has merits and problematic issues. A relatively new coupling approach uses compliant elastomer films, where upon contact the surfaces of probes and parts mate sufficiently (the film conforming around contacting asperities that normally cause gaps) to couple the sound from one to the other with reasonable efficiency. If complete coupling is not achieved, only a very small amount of other coupling agents (oil, water, gel, or condensate inside a pipe) can restore the desired coupling condition.

Few ultrasonic probe manufacturers produce dry-coupled ultrasonic probes, and even fewer produce so-called “wheel probes” that are seen as particularly useful in a scanning (moving inspection) application, and the proprietary elastomer films are closely held secrets. Dry coupled probes are limited to moderate frequencies (below immersion upper ranges and above air-coupled limits) and certainly within the range useful for polymer inspections. The designs of dry-coupled wheel probes commercially available would allow all manner of ultrasound to be used (focused and unfocused, angle beams and various modes), but in some cases would require probe pairs (two probes inside a single wheel or two wheels) instead of single probes.

Application in plastic pipe inspections

The use of dry-coupled probes, and in particular dry-coupled wheel probes, is seen as a very promising application for plastic pipe inspections. Because the similar acoustic impedance of the dry-coupling elastomer film and the polyethylene pipe, transmission losses are minimized, and the fact that no other coupling media is needed to be supplied during inspection makes deployment much simpler. As noted, it is likely that any condensate present in the pipe would only serve to enhance coupling, provided the chemical make-up of the condensate does not cause deterioration of the dry-coupling film. An added benefit of a wheel probe is the rolling contact of the coupling

patch, which will minimize drag forces for any scanning system. The wheel probe may be spring loaded in a design akin to a trailing arm to allow the probe to swing out of the way of smaller obstacles within the pipe passively instead of needing active mechanical means to lift the probe out of the way of obstacles. Reliability in the rolling wear performance of the elastomer films for scanning thousands of feet of piping needs to be established. Finally, size is a concern, as those dry-coupled roller probes currently on the market are certainly large for the pipe dimensions covered in this project, requiring more robot modules to produce full coverage inspection of the pipe.

Microwave

How it works

Microwave and millimeter-wave synthetic aperture radar (SAR) 3D imaging utilize electromagnetic signals in the frequency range of ~300 MHz to 300 GHz, corresponding to a wavelength range of 1000 mm to 1 mm. In general, as frequency increases 'resolution' increases and the feature size that can be detected becomes smaller, meaning that microwave techniques can detect relatively small anomalies and flaws [1, 2]. Signals at these frequencies easily penetrate inside dielectric materials such as Polyethylene (PE), providing high resolution images of their inner structures. Additionally, microwave signals are sensitive to changes in the dielectric properties of the materials enabling accurate material characterization [1, 2].

Microwave Imaging techniques are conducted primarily using raster scanning, although in lieu of mechanical (raster) scanning, 1D and 2D arrays of antennas can be assembled, to perform rapid electronic scanning. The collected data (by scanning or using the array) is then mapped directly to a contrast image or processed using backpropagation algorithms such as the synthetic aperture radar (SAR) [2]. Thus, the choice of imaging technique, probe type, and frequency of operation are dependent on the sample properties and the target features (e.g., crack, void, delaminations, etc.).

Advanced and unique millimeter-wave imaging systems have been designed for NDE applications. An example of such system is a *real-time, portable, high-resolution* and 3D imaging microwave camera operating in the 20-30 GHz frequency range [3]. For detailed description of microwave NDE technique, interested readers are referred to [2].

Application in plastic pipe inspection

As mentioned above, microwave signals can penetrate dielectric materials such as high density polyethylene (HDPE) and interact with their inner structures. Therefore, microwave signals are capable of detecting various defects in PE pipes including delamination, gauges and presence of foreign material [4-6]. Microwave signals are air coupled allowing for scanning the target from a large standoff distance allowing for implementation of a contactless sensor array on a robotic platform for pipe inspection. Furthermore, with the advancement of system-on-chip radar sensors, it is possible to construct small size and low-power sensor arrays.

Online monitoring of HDPE pipes carrying natural gas is enabled since gas composition (or other materials in gaseous form) does not affect microwave testing. Microwave sensors are typically not sensitive to moderate levels of moisture. However, pooled liquids and solids on the

surface of the pipe will interfere with the microwave signals.

In summary, microwave signals are air launched and do not require contact between sensors and the pipe wall. Furthermore, commercial-off-the-shelf system-on-chip radar sensors can be readily configured as a small, low weight, and low power imaging array carried by an inspection robot allowing for online monitoring of gas pipeline.

References

1. Zoughi R. Microwave Non-Destructive Testing and Evaluation Principles: Springer Netherlands; 2000.
2. Brinker K., Dvorsky M., Al Qaseer M. T. and Zoughi R., "Review of advances in microwave and millimeter-wave NDT&E: principles and applications" Phil. Trans. R. Soc. 2020, 378, 20190585-20190585 <http://doi.org/10.1098/rsta.2019.0585>
3. Ghasr M. T., Horst M. J., Dvorsky M. R. and Zoughi R., "Wideband Microwave Camera for Real-Time 3-D Imaging," IEEE Transactions on Antennas and Propagation, vol. 65, no. 1, pp. 258-268, Jan. 2017, doi: 10.1109/TAP.2016.2630598.
4. Carrigan TD, Forrest BE, Andem HN, Gui K, Johnson L, Hibbert JE, et al. Nondestructive Testing of Nonmetallic Pipelines Using Microwave Reflectometry on an In-Line Inspection Robot. IEEE Transactions on Instrumentation and Measurement. 2019;68(2):586-94.
5. Laviada J, Wu B, Ghasr MT, Zoughi R. Nondestructive Evaluation of Microwave-Penetrable Pipes by Synthetic Aperture Imaging Enhanced by Full-Wave Field Propagation Model. IEEE Transactions on Instrumentation and Measurement. 2019;68(4):1112-9.
6. Ghasr M. T. & Gao Y. & Zoughi R. , (2019) "Handheld microwave imaging system for the inspection of non-metallic structures", *Review of Progress in Quantitative Nondestructive Evaluation* 0(0)

Terahertz

How it works

Terahertz imaging and spectroscopy (collectively THz in short) is one of the newest and most promising technological additions to the NDE tool box for material inspection and characterization. THz utilizes the electromagnetic energy radiated in the frequency range from 50 GHz to 10 THz and up, generally in-between microwave and mid-infrared. THz can penetrate many common gases, non-metallic solid and non-polar liquid, and also possesses distinct spectral characteristics in water vapor, polar plastics, certain gases, DNA samples, crystalline solid and explosives. All these advantages make THz particularly applicable in the areas of automotive, aviation, food and consumer, pharmaceuticals, medical diagnosis, defense, and homeland security. The research team at CNDE has also enjoyed great success in addressing the inspection problem of the space shuttle external tank foam insulation [1-2], the inspection of Army's advanced ceramic materials and their encapsulated armor structures for personnel and vehicle protection [3], as well as providing assistance in Air Force Research Laboratory's THz development [4-6].

The various ways of THz generation and reception include frequency down conversions involving lasers (such as photoconductive antenna, electro-optical sampling and photomixing), frequency up conversions involving microwave (such as backward wave oscillator, Schottky diodes with frequency multiplication) and other sources (such as gas laser, quantum-cascade laser, free electron laser) and sensors (such as bolometers, Golay cells, pyroelectric devices) (see, e.g. [7]). By taking the popular photoconductive antenna approach, THz pulses in high repetition rate can be reliably generated for raster scanning parts of interest. To this end, THz works operationally like high-definition ultrasound without the need of coupling medium and the general limitations of mechanical wave. A-, B- and C-scan data are now routinely acquired with superb quality.

Application in plastic pipe inspections

With its exceptional temporal and spatial resolution, THz is a great match for inspecting plastic pipelines. As demonstrated from the ongoing NYSEARCH-funded project, THz can detect and size indications of 0.5mm diameter or smaller embedded in the pipe wall and can resolve the delamination layers of the real Driscopipe8000 pipe samples extracted from the field. From the preliminary testing in the current DOT/NYSEARCH Phase 1 project, THz was also shown capable of differentiating different backing on the outer surface of pipe as well as different formation of simulated delamination, inspected from the inside of pipe through 1-inch pipe wall thickness. One unique advantage of THz over other NDE techniques is its potential of performing *spectroscopic imaging*. If the spectral fingerprints do exist, THz might be able to simultaneously detect (via imaging) the various defects on or within pipe body and assess (via spectroscopy) the joint composition and bonding strength.

Given THz's short history in the field of NDE, THz equipment is relatively larger in size and costlier in development than other matured NDE techniques. Thanks to recent advances in optoelectronics, fortunately, affordable commercial systems have rapidly appeared in market to make THz technology much more accessible [8]. Miniaturization of THz sensors is now within reach to work inside of pipe of 4-6-inch diameter, as demonstrated in progress made in the current project. In addition, work is underway to significantly improve the scan speed by considering array approach that has been commercialized recently [9].

References

1. C.-P. Chiou et al., "Modeling and processing of terahertz Imaging in space shuttle external tank foam inspection," in Review of Progress in Quantitative Nondestructive Evaluation, 2006, Vol. 25A, pp. 484-491.
2. C.-P. Chiou et al., "Processing terahertz ray data in space shuttle inspection," in Review of Progress in Quantitative Nondestructive Evaluation, 2007, Vol. 26A, pp. 425-431.
3. C.-P. Chiou et al., "Nondestructive characterization of UHMWPE armor materials," in Review of Progress in Quantitative Nondestructive Evaluation, 2012, Vol. 31B, pp. 1168-1175.
4. C.-P. Chiou, R. B. Thompson and J. L. Blackshire, "Modeling of terahertz ray signals for NDE applications" in Review of Progress in Quantitative Nondestructive Evaluation, 2008, Vol. 27A, pp. 414-420.

5. C.-P. Chiou, J. L. Blackshire and R. B. Thompson, "Terahertz ray system calibration and material characterizations," in Review of Progress in Quantitative Nondestructive Evaluation, 2009, Vol. 28A, pp. 410-417.
6. C.-P. Chiou et al., "Signal modeling in the far-infrared region for nondestructive evaluation applications," in Review of Progress in Quantitative Nondestructive Evaluation, 2011, Vol. 30A, pp. 581-588.
7. P. H. Siegel, "Terahertz Technology," IEEE Transactions on Microwave Theory and Techniques, Vol. 50, No. 3, March 2002.
8. A. Redo-Sanchez et al., "Review of Terahertz Technology Readiness Assessment and Applications," J Infrared Milli TeraHz Waves (2013) 34:500–518 DOI 10.1007/s10762-013-9998-y.
9. World Leading Terahertz Solutions | TeraView (<https://teraview.com/>).